FLUVIAL RESPONSE TO GREAT SALT LAKE LEVEL CHANGES: OBSERVATIONS, MECHANISMS AND IMPLICATIONS

by

Krysia Wade Skorko

A thesis submitted to the faculty of
The University of Utah
in partial fulfillment of the requirements for the degree of

Master of Science

in

Geology

Department of Geology and Geophysics

The University of Utah

May 2010

THE UNIVERSITY OF UTAH GRADUATE SCHOOL

SUPERVISORY COMMITTEE APPROVAL

of a thesis submitted by

Krysia Wade Skorko

This thesis has been read by each member of the following supervisory committee and by majority vote has been found to be satisfactory.

Chair: Paul W.

THE UNIVERSITY OF UTAH GRADUATE SCHOOL

FINAL READING APPROVAL

To the Graduate Council of the University of Utah:

I have read the thesis of Krysia Wade Skorko in its final form and have found that (1) its format, citations, and bibliographic style are consistent and acceptable; (2) its illustrative materials including figures, tables, and charts are in place; and (3) the final manuscript is satisfactory to the supervisory committee and is ready for submission to The Graduate School.

Paul W.
Chair: Supervisory Committee

Approved for the Major Department

D. Kip Solomon
Chair/Dean

Approved for the Graduate Council

Charles A. Wight
Dean of The Graduate School

ABSTRACT

A better understanding of fluvial adjustments to base level changes may benefit the fields of sequence stratigraphy, geomorphology and petroleum geology. This investigation provides a modern case study of the channel evolution of the Lee Creek and the Goggin Drain, two streams that flow into the Great Salt Lake, a lacustrine system that experiences rapid base level changes. Using aerial images, fieldwork and LiDAR data, a detailed study of geomorphology and channel hydraulics was conducted for the purpose of explaining variations in channel form and avulsion behavior. While Lee Creek, a meandering system, has not recently been avulsive, three major avulsions of the Goggin Drain have taken place since 1965. During this time, lake levels fluctuated from near their historic lowstand to their historic highstand, an elevational difference of more than 6 m, and again approach lowstand in the present. Two possible styles of avulsion are interpreted: an allogenic response to changing base level, and an autogenic response dictated by channel morphology and hydraulics. Despite a wealth of available information for this system, avulsions cannot be positively attributed to one style or another; caution should be used when attempting to link the complex process of avulsion to causal mechanisms.

TABLE OF CONTENTS

LIST OF TABLES

ACKNOWLEDGEMENTS

Many thanks to the many people who have been so helpful during this process. Thank you to my committee, Paul Jewell, Kathleen Nicoll and Cari Johnson, for all your advice and assistance. For funding, I would like to thank the University of Utah Seed Funding Grant and the National Science Foundation GK-12 program (WEST). Thank you to Anne Neville of Kennecott Copper/Rio Tinto and to Ella Sorensen of the Audubon Society for advice and access to field sites. Thank you to Neil Lareau, in particular for assisting with fieldwork, and in general for helping me along every step of the way. I would also like to thank my friends, family and fellow students for their support.

CHAPTER 1

INTRODUCTION

Changes in base level and the subsequent effects on stratigraphy have become the basis for the development of sequence stratigraphy, and are of great importance to the field of sedimentary geology and geomorphology. However, the nature of fluvial responses in this context has long been a controversial topic, and is often misunderstood and sometimes oversimplified. Isolating the effects of base level changes is difficult, as changes in natural systems are invariably linked to several factors (Miall 1996). Deconstructing these complex reactions through laboratory experimentation, numerical modeling and field investigations have become topics of recent interest. This study aims to investigate a subset of this topic – the relationship among geomorphology, channel avulsions and base level change – through an investigation of a modern system.

Prior studies in geomorphology, sequence stratigraphy, alluvial architectural modeling and related fields of geology have noted the lack of data on modern channel avulsions and what causes them (Hart & Long 1996). This study aims to contribute a modern case study of an avulsive fluvio-lacustrine system. Specific goals are 1) to reconstruct the history of fluvial adjustments and channel evolution of two streams, the Lee Creek and Goggin Drain, in response to Great Salt Lake level fluctuations, 2) to assess the possible causes of avulsion of the Goggin Drain through analysis of

geomorphology and channel hydraulics, and 3) to assess the effectiveness of a relatively new technology, LiDAR, as an interpretive tool for this type of study.

Fluvio-Lacustrine Systems and Terminal Basins

There has been recent interest and research in applying the concepts of marine sequence stratigraphy to lacustrine basin settings, motivated by the prospect of finding economic and productive hydrocarbon reserves (Lin et al. 2001). Using subsurface and outcrop data, stratigraphy within nonmarine closed basins has been a subject of increasing interest. (Keighley et al. 2003). A modern study of base level changes in fluvio-lacustrine systems could benefit this field of research, and develop a greater understanding of linkages between form, process, and the resulting sequence architecture. Additionally, this type of study may be especially useful as a way of documenting the sedimentary response to a base level drop, a modern marine condition uncommon in the modern marine environment, unless tectonically induced. Because most systems that are readily interpreted are Holocene to modern, a time period that was characterized by rising sea levels, the fluvial response to regressive changes has mostly been inferred from ancient systems or modeling. The link between regressive processes and stratigraphy is therefore limited (Hart & Long 1996).

The Great Salt Lake provides a unique environment to study the fluvio-lacustrine system in response to base level changes. Because the offshore bathymetry has a gentle slope, relatively small changes in lake level can cause a rapid lateral migration of the shoreline, and these changes to the system have been well documented. As water levels have fluctuated, fluvial adjustments, including channel avulsions, have been documented with aerial imagery. Lake and stream hydrographs, aerial photos, satellite images and

high resolution LiDAR digital elevation models are readily available for a decadal time scale.

Fluvial adjustments to base level changes have been studied in environments similar to the Great Salt Lake. An analog is the Volga Delta, a larger river system that wanders greatly as Caspian Sea levels fluctuate. For this reason, the sedimentary architecture of this delta differs strongly from other large deltas, and is not well understood (Kroonberg et al. 1997). Hassan and Klein (2000) have investigated fluvial adjustments of the Jordan River as it flows into the receding Dead Sea. However, these studies do not discuss modern channel avulsions in detail. The study with a field site perhaps most similar to the Great Salt Lake is Blair and McPherson's (1994) study of historical adjustments of the Walker River due to the fluctuations of Walker Lake, where 12 separate deltas formed as a result of lake's shoreline regressions and tectonic tilting of the lake bed since 1882. A study of the Great Salt Lake also serves as a case study of a unique system in which changes can be well documented.

Fluvial Processes - Channel Avulsions

Channel response to base level changes often takes the form of an avulsion, which is defined as the process whereby a channel belt shifts abruptly from one location to another in favor of a new gradient. The channel may reoccupy a preexisting channel or take a new path, which typically evolves from a crevasse splay (Bridge 2003). However, this response can be complex and difficult to predict. Avulsion most commonly occurs during flooding events, but several factors can increase the likelihood for a stream to reach its avulsion threshold. Flume and field studies have showed that both the rise and fall of base level can shift a system towards its avulsion threshold (Jones & Schumm

1999). Factors relating to base level change include the rate and amount of change, increases in sediment supply, channel blockage, and, in the case of base level drop, the geologic and geomorphic properties of the newly exposed land area, such as the slope, sediment type, bedrock and structural controls (Jones & Schumm 1999; Bridge 2003). For example, falling base level may lead to a decreased gradient of the newly exposed shelf, leading to sediment deposition and channel blockage. This scenario is often applied to delta progradation, or to instances when the newly exposed slope is a flat lake bed. A study of the Saskatchewan River attributed major avulsions to an abrupt decrease in slope as the river enters the flat lacustrine plain of former Lake Agassiz (Morovosa and Smith 1999). A rise in base level may reduce slope, causing similar aggradational conditions and increasing the potential for avulsion (Schumm 1993). While the causes of avulsion are sometimes attributed to external forcing, such as tectonic tilting, climate and base level changes, or flooding, other studies have suggested that avulsion is a purely autogenic, or self-generated, response (Miall 1996).

Avulsions of the fluvial system have received the attention of researchers due to their importance in stratal architecture modeling. These studies have shown that avulsions are a key factor in how fluvial systems create sand channel body deposits, which form hydrocarbon reservoirs, aquifers, host economic minerals, and are therefore of high economic importance (Gibling 2006). Avulsion frequency and sedimentation rate have been shown to be the primary factor controlling the density and interconnectedness of these channel bodies, a major factor in the productivity of oil reservoir (Hickson 2005).

Previous Work on the Causes of Avulsion

Physical Modeling

The causes of channel avulsions, especially in relation to base level changes, have been largely investigated through laboratory flume experiments. Much of the early influential work, beginning in the 1970s and continuing through the 1990s, was conducted at flume facilities at Colorado State University. This work, summarized in detail by Ethridge et al. (2005), has led to much of what is known about alluvial channel dynamics.

Further research has been conducted through the ongoing work at the University of Minnesota. Their facility, which is used to simulate large scale basin development, is called the Experimental Earthscape (XES), also referred to as "Jurassic Tank". The facility at St. Anthony Falls Laboratory is a large flume with a basin floor that can simulate subsidence. This experimental setup provides a means for analyzing the stratigraphic development of a basin while precisely controlling sediment and water supply, subsidence and base level change (Heller et al. 2001).

A significant challenge in relating laboratory results to natural systems is the issue of scale. Determining what scale these simulations represent remains in question. Additionally, the problem of processes that cannot be scaled in a simple manner, such as fluid viscosity and grain size, must be considered before laboratory modeling results can be accurately applied to actual depositional systems (Hickson et al. 2005).

Field Investigations

While much of the study of relationship between base level change and avulsion has taken place in flume experiments, several field investigations of avulsive channels have been conducted over a variety of timescales ranging from the Jurassic to the Holocene and modern systems (Aslan & Blum 1999; Bristow 1999; Ethridge et al 1999; Morovosa & Smith 1999; Sinha et al 2005; Stouthamer & Berendsen 2000, Stouthamer & Berendsen 2007). Several of these studies deal with re-creating avulsion histories, often using hundreds to thousands of borehole samples, aerial images and outcrop data. Some attention has been focused on understanding the response of the fluvial system in relation to base level, tectonic or climatic forcings, such as a study by Stouthamer and Berendsen (2000). Using data from thousands of boreholes and radiocarbon dates, they re-created the Holocene avulsion history of the Rhine-Muese river system and related their results to observed sea-level changes. A modern avulsion of the Niobrara River, Nebraska, occurring in 1995 was attributed to being pushed to near its avulsion threshold by years of aggradation due to a 2.9 m base level rise caused by the damming of the Missouri River (Ethridge et al. 1999).

Other field investigations have noted the autogenic nature of avulsions, such as those observed in the Kosi River, India. As summarized by Miall (1996), many studies have demonstrated that the avulsive shifts observed in the Kosi fan were not related to major flood or tectonic tilting, but were entirely autogenic.

Numerical Modeling

Alluvial architecture models have been developed as a way of investigating how external controls on the fluvial system may be recorded in the sedimentary record. The

purpose of this research is to produce models that proposed clear, testable predictions regarding the interplay of several factors within the system (Hickson et al. 2005). This was spearheaded by Leeder in a 1978 paper proposing the relationship between the depositional stacking of channel belt deposits as a function of avulsion and sedimentation. This work has continued with a series of papers by Allen, Bridge, Alexander and other co-workers. For convenience, following Heller and Paola (1996) and Hickson et al. (2005), this series of work is collectively referred to as the LAB (Leeder, Allen & Bridge) models.

The essence of the original LAB model is that architectural stacking is mainly dependant on avulsion frequency, sedimentation rate, and the ratio between channel belt width and basin width, and variation in these factors will result in changes in channel belt stacking patterns (Hickson et al. 2005). This model has been applied by the petroleum industry as a way to predict the interconnectedness of sand bodies, which is linked to the productivity of oil reservoirs. A later model by Bride and Mackey (1995) created a similar model in three dimensions. Heller and Paola's 1996 model draws from similar principles, and also to explains downstream changes in stratal architecture, in which sedimentation rate varies with systems tract position. Results show that the rate of downstream changes is primarily dependant on sedimentation rate, but the style of change (increase or decrease) of stacking densities is dependant on avulsion frequency and avulsion type (Heller & Paola 1996). A more recent study by Hickson et al. (2005) has involved re-creating the architecture predicted in the early LAB models using physical modeling techniques at the Experimental Earthscape Facility at the University of Minnesota.

Research Justification

A greater understanding of avulsion processes could benefit the fields of geomorphology, sedimentology, stratigraphy and petroleum geology. Despite the various studies of avulsion history, our understanding of the controls of avulsions, and the resulting stratigraphic effects, remains incomplete (Morovosa and Smith 1999, Kraus & Wells 1999). This is mainly due to insufficient data linking causal mechanisms to specific avulsion events (Stouthamer and Berendsen 2001). Whole-channel avulsions are rare events in nature, and are a poorly understood process. There are few observational data on the process, and more quantitative field observations are needed. Field data on changes in avulsion frequency are hard to come by, because these events are too infrequent to yield meaningful statistical trends of average rates. Also, it is difficult to reproduce some common natural systems, such as muddy rivers, in a laboratory model or flume experiment (Heller and Paola 1996).

More research on the processes controlling avulsion, especially in relation to base level changes, would benefit the subject of alluvial architectural modeling. Some general conclusions that have been drawn from these models are 1) that variation in stratal architecture is strongly controlled by sediment supply and base level change, and 2) that all alluvial architecture models are limited because little is known about the processes controlling sand body stacking and avulsion. Until a complete relationship of avulsion processes is developed, stratal architecture models should be considered as working hypotheses only (Heller and Paola 1996).

LiDAR as a Tool in Fluvial Geomorphology

Useful data for fluvial systems may be collected with LiDAR (Light Detection and Ranging), a remote sensing technique capable of producing highly accurate digital elevation models. With this method, laser pulses are emitted from an aircraft or ground-based apparatus and reflected back to a receiver. The time between emission and detection is converted to distance, and thousands of these pulses are used to create a digital elevation model (DEM). These are much more accurate than traditional DEM's, and are generally accurate to 50 to 100 cm in the horizontal direction and 10 to 15 cm in the vertical direction. LiDAR is especially useful to geomorphologists because a 'bare earth" model can be created by using only final laser returns, thereby eliminating vegetation (Moskal 2008). Previous studies of fluvial systems (Thoma et al. 2005; Hilldale & Raff 2007) have recognized the value of replacing time-intensive field techniques with LiDAR analysis, but more research is needed in order to determine how effective this may be. While these DEMs have the potential for great success in improving the visualization of landscape processes and changes, they also pose new technical challenges in data processing and computation (Snyder 2009).

Study Site – The Great Salt Lake

Both the Lee Creek and Goggin Drain are part of the Jordan River watershed and flow toward a base level in the Great Salt Lake north of the town of Magna. Both streams flow through industrial areas, and their channel forms are artificially controlled over most of their longitudinal profile, and flow through cement-banked canals. About 2 km from the present Great Salt Lake shoreline, river channels are no longer controlled and allowed

to flow unrestricted into the lake. The study area for this project focuses on the lower reaches of these streams, between the transition from artificial to natural channels and the flow terminus along the Great Salt Lake (Figure 1.1).

Within the study area, the two creeks share some geomorphic and geologic characteristics. The terrain they flow through is very flat, with overall stream gradients on the order of 1 to 2 m per kilometer. These are alluvial channels, with substrates composed of Lake Bonneville muds, including resistant caliche layers. The study area is a sagebrush-steppe and halophyte ecosystem, sparsely vegetated except for reeds that occur along the banks of these streams in thick patches. Both streams have experienced recent incision up to 2 m with the drop in lake level, which is deepest in the middle reaches of the study areas.

The Lee Creek drains the area north of a Rio Tinto (formerly Kennecott Copper) tailings pond, and is channelized in most of its upper reaches. Upstream of the USGS gauging station (Figure 1.2), which marks the beginning of the study reach, the creek does not appear to be channelized – it flows through broad marshes which are engineered wetlands. In the vicinity of the gauging station, the flow quickly converges into a channel, which is unconstricted from this point to the lake. Lee Creek is the smaller of the two streams in the study, with maximum discharges reaching about 2.5 m^3/s. It is a single threaded, slightly sinuous channel with two major nickpoints, one of which is a human-made rock barrier. About 400 m downstream of the gauging station, there is a natural nickpoint which takes the form of a small waterfall, which has eroded 140 m headward over a 6 month observation period. Three geomorphically distinct reaches of the stream within the study area can be defined, characterized by their channel form, roughness,

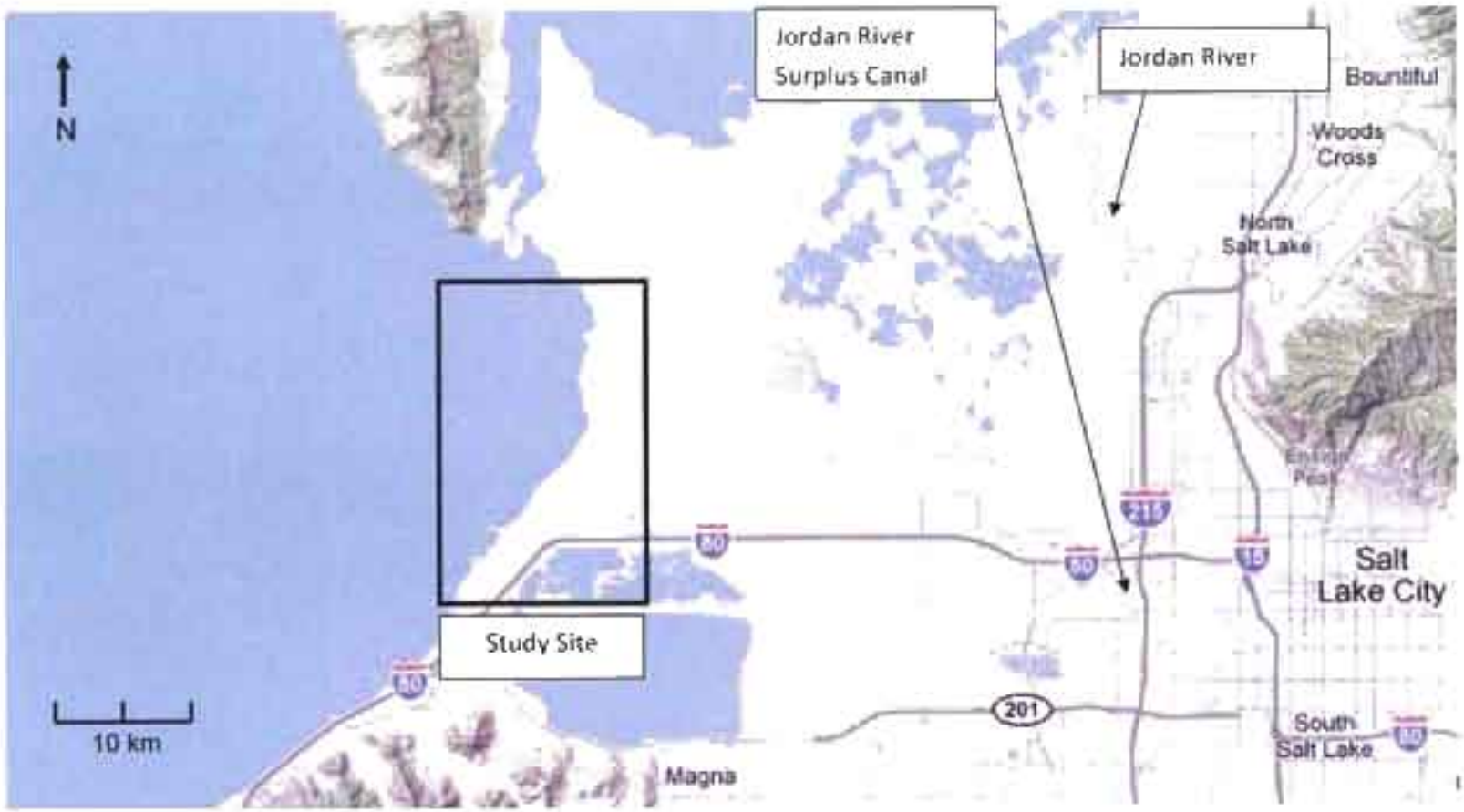

Figure 1.1 Google Maps image of the study area.

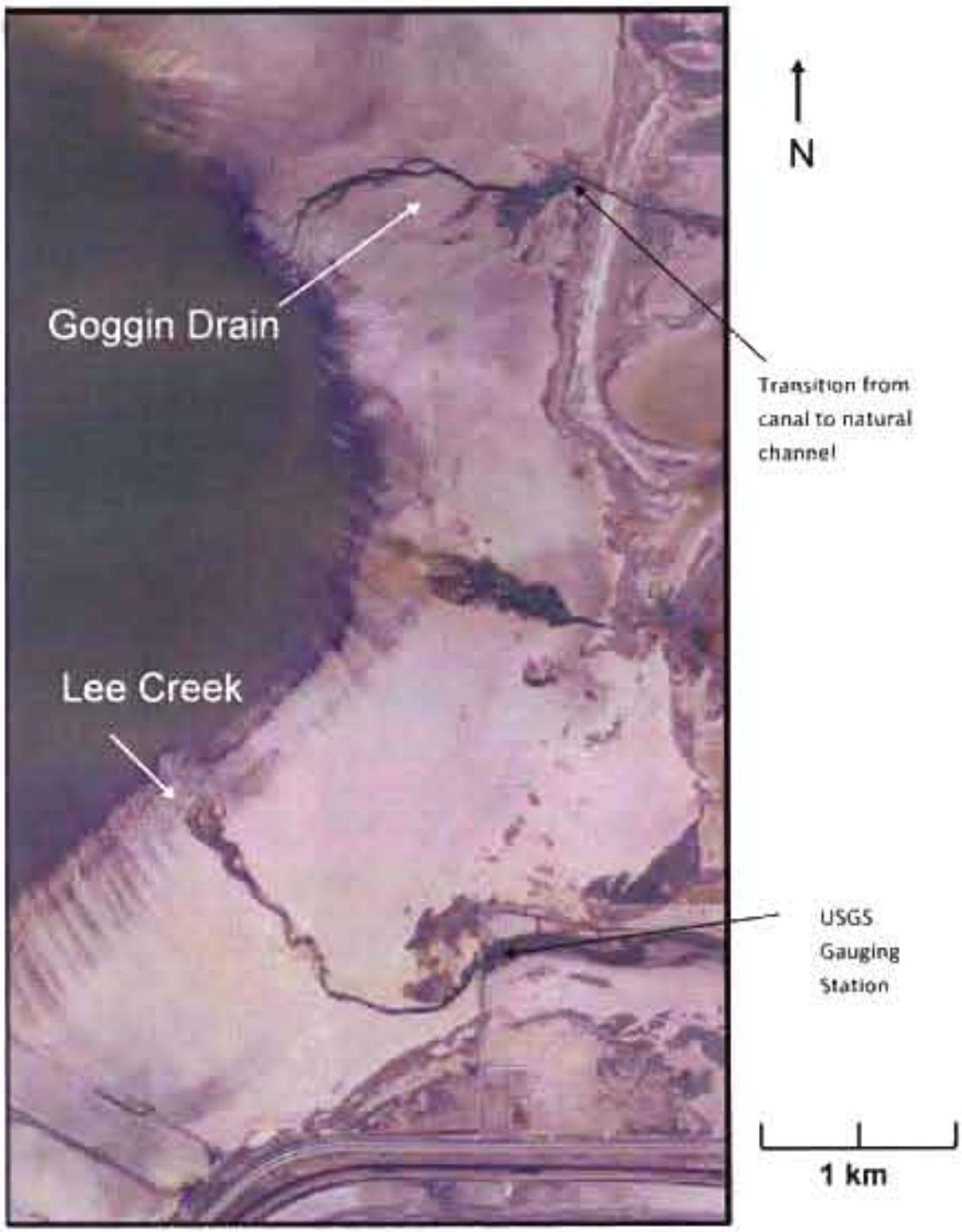

Figure 1.2. 2006 aerial photograph of the Lee Creek and the Goggin Drain.

incision depth and presence of vegetation. These geomorphic reaches are described in greater detail in Chapter 3: Results.

For most of its course, the Goggin Drain is an engineered stream designed to control flooding of the Jordan River Surplus Canal by diverting excess runoff to the Great Salt Lake. Its form is a structurally controlled canal that is released above the modern lakeshore, below which it flows naturally into the lake. The natural section of the channel is geomorphically similar to the Lee Creek in that has incised upper reaches and a distributary lower section. Its major differences are that unlike the Lee Creek, incision appears to have taken place over the entire length of the study site, and that it is much larger than the Lee Creek, with maximum discharges reaching ~ $45m^3/s$. Also, there are few stretches of the Goggin that flow as a single threaded channel, and there are no falls or nickpoints observed. The main channel is surrounded by large remnant channels, some of which appear to be the result of complete avulsions, as they do not rejoin the modern channel. This creek has three main geomorphic reaches, which are described in more detail in Chapter 3: Results.

CHAPTER 2

METHODS

Historical Analysis

To recreate the avulsion history of the Lee Creek and the Goggin Drain, aerial photographs and satellite images of the area were collected from various sources, including the Utah AGRC (Utah Automated Geographic Reference Center) and the IRDIAC (Intermountain Region Digital Image Archive Center). These images clearly display the channel forms and lake levels over time. Lake levels and stream flow measurements are available through the USGS, which displays both lake and stream hydrograph information on their website, http://ut.water.usgs.gov/. The hydrographs for both streams are missing many years of data due to the lake highstand, so to investigate the potential for flooding in the Goggin Drain, the hydrograph for the nearby Jordan River Surplus Canal was used as a proxy.

Geomorphic Analysis

LiDAR Analysis

Between the years of 2006 and 2008, the entire Wasatch front and surrounding areas were mapped as part of an airborne LiDAR survey. This project was a joint effort by several agencies including local government, the USGS, the Utah Geological Survey and the Utah Automated Geographic Reference Center (AGRC). LiDAR digital elevation

models of the area are available through the Utah AGRC and may be downloaded from their website, http://agrc.its.state.ut.us/. The DEM of the Lee Creek and Goggin Drain used for this study is a 1.25 m gridded bare earth model, which was developed from datasets flown in October of 2006. For a portion of the Goggin Drain, a terrestrial LiDAR survey was conducted in November of 2007. Both datasets were analyzed with ArcGIS software to create-cross sectional and longitudinal profiles, topographic contours examine sedimentary features and to measure distances, areas and volumes. Due to the high resolution of these images, the LiDAR data captured subtle low-gradient sedimentary features that were not visible in the field or on aerial photographs. Experimenting with ArcMAP's visual effects, such as color ramping and hillshading, reveals many features of interest.

Longitudinal profiles were created by using the ArcGIS 3D Analyst line interpolation tool, which displays an elevational profile of any line drawn across a DEM. Because of sparse returns over surface water, stair-step patterns were initially produced with this method. Connecting the minima in these profiles provides an accurate representation of stream channel profiles (Snyder 2009). Channel profiles were produced in this manner, along with profiles of the land surface along the channel banks.
Cross sectional profiles were also created using ArcGIS 3D Analyst. To capture the topography of the banks, the location of these profiles was chosen carefully in order to avoid thick patches of vegetation. Because of voids in the data over the water-filled stream channels, the elevation of the water surface was corrected to be consistent with the water surface elevations calculated from the longitudinal profiles.

The LiDAR data were used to infer the lake level at the field site during the mid-1980s highstand. No aerial photographs or satellite images were available from this timeframe, but because the lake levels are known through the USGS gauging station, a contour at this level could be added to the dataset to show the extent of the shoreline during this time.

Field Methods

Fieldwork was conducted for the purpose of ground truthing the LiDAR data, classifying reaches according to geomorphic features, and to conduct incision measurements. Field measurements of incision depth were necessary for calculating velocities and estimating sediment volumes.

Incision was measured at several points along the channels, with each measurement representing the most upstream point of a reach with a similar degree of incision, width and depth. Total incision depth, or the distance from the uppermost bank to the channel bed, was measured by an onshore observer sighting a stadia rod which was being held in the deepest part of the channel. The height of the observer's eye level was then subtracted. The depth of the water at each point was also recorded, and this was used to calculate the incision from the top of the bank to the water surface. Measurements were taken starting upstream and working down, and were taken wherever incision changes were noticed. This technique was used for the entirety of the Lee Creek. However, due to high flow conditions at the time of fieldwork, water depth measurements could not be taken for the Goggin Drain in a similar fashion. Instead, incision from the water surface to the top of the bank was measured, and water depth and

total incision depth were either derived from the terrestrial LiDAR data or from averages of available measurements.

These incision measurements were used to calulate sediment volumes removed from the current channel. Based on LiDAR cross sections and field observations, the channel bed of these streams was assumed to be rectangular, and segments could therefore be simplified into rectangular prisms. Measuring the length of these segments in ArcMap allowed their volume to be easily calculated. Summing the segment volumes then accounted for the volume of sediment removed by channel incision.

The LiDAR and field investigations of the area provided the necessary information to characterize channel reaches according to geomorphology. The channels were divided into distinct geomorphic reaches that are internally similar in form and other characteristics. Designation of reaches was important in calculating velocities using the Manning equation, as the water depths, widths, and gradients measured within each reach were averaged in order to simplify these calculations.

Quantitative Methods

The Manning equation for average cross-sectional velocity was applied to singe-threaded reaches of the channels. This empirical equation relates channel dimensions, roughness and slope to flow velocity as a way of understanding erosive changes both spatially and temporally.

The Manning equation for velocity within the channel is as follows:

$V = k/n\ R^{2/3}\ S^{1/2}$ (Equation 2.1)

Discharge can then be calculated:

$Q(m^3/sec) = V(m/sec)A(m^2)$ (Equation 2.2)

where V = cross-sectional velocity (m/sec)

k = 1.0 for SI units and 1.486 for English units

R = hydraulic radius = Area (m^2)/Perimeter(m)

n = Manning coefficient for channel roughness

S = channel slope or gradient (m/m)

Q = discharge (m^3/sec) = (cross-sec. velocity (m/sec)) (cross sec. area (m^2))

(Bloom 1998)

The hydraulic radius of the channel (R) is found by dividing the area of the wetted channel by the wetted perimeter. Assuming a rectangular channel, area and perimeter measurements were easily calculated. Slope was determined using the airborne LiDAR data. The channel roughness coefficient (n) is typically calculated through Cowen's method or can be estimated based on channel characteristics (McCuen 1998). In this case it was calculated from the known variables of Equation 2.2. Because the discharge (Q) at the time of the measurements was known through stream gauge measurements, roughness (n) becomes the only unknown variable in the equation, and was adjusted until obtaining the proper value for discharge.

For Lee Creek, the velocity in each geomorphic reach was assessed. Velocity was calculated only for the canal portion and reach 1 of the Goggin Drain. This is because

reaches 2 and 3 are not single-threaded channels, and therefore the Manning equation does not apply. Because a large portion of reach 1 was covered by the terrestrial LiDAR survey, the velocity calculations were based on these data rather than on field measurements.

Water velocities within the channelized portion of the Goggin Drain were investigated by applying the Manning equation, and using parameters known from the USGS gauging station as input. Again the channel was assumed to be rectangular, and the same measurements were needed to calculate velocity – depth of water, width of the channel, gradient and roughness. In this case water depth was taken from the USGS gauge height of the canal. This was a necessary step because the canal was too deep to measure water depth manually. On the USGS website, records are available for the relationship between some discharges to gauge heights, which were plotted against each other. A curve was fit to this plot by using the Manning equation to calculate discharge for a series of gauge heights, which was adjusted to the best fit by changing the roughness coefficient, which was the only unknown variable. By selecting the roughness coefficient that fit the relationship best, the Manning equation could then be used to calculate velocities within the canal. These velocities were then compared to those within the natural portion of the channel.

For each of the streams, the velocity was initially calculated for one discharge. Because rectangular channels were assumed, velocity could be calculated over the full range of discharges by simply varying the water depth. For each water depth, the hydraulic radius, slope and previously calculated roughness coefficient could be found

and used to calculate velocity, which was then multiplied by the cross-sectional area of the channel to find discharge.

In order to get assess the accuracy of the Manning velocity calculations, field measurements of velocity were conducted for comparison. Ideally, velocity would have been measured in each of the geomorphic reaches of both creeks. However, because of high water conditions in the incised regions of the channels, field measurements were only attainable for the first and third geomorphic reaches of the Lee Creek. A Pygmy flow meter was used for these measurements. This method involves counting the number of revolutions over a predetermined time period, and then converting revolutions per unit time to velocity. By repeating these measurements over a representative cross section of the creek, the cross-sectional area and total discharge can be measured, and then the average cross-sectional velocity can be calculated by dividing the discharge by the area (Sanders 1998). Measurements were taken in 0.6 m (2 ft) increments.

The measured discharge was used to calculate a theoretical velocity from the Manning equation. Because the Lee Creek gauging station was not functional at the time of measurements, the field calculated discharge was assumed to be correct. The calculated and observed velocities corresponding to this discharge could then be compared.

For the Lee Creek, a meandering system, empirical relationships between, width, discharge, and meander length were compared. These equations are summarized by Bridge (2003). Inputs for these equations are average widths and meander lengths measured in ArcMAP, and average discharge reported by the USGS gauging station.

CHAPTER 3

RESULTS

History of Lake Level Changes and Fluvial Adjustments

Aerial Image Interpretation

Aerial images of the study site were compiled from the earliest available, 1965, to the present. Aerial photographs were compiled from 1965, 1971, 1977, 1980, 1997 (months taken are unknown) and October 2006. Satellite images were found for April 2001, June 2005, and September 2005. During this time period, the water levels of the Great Salt Lake underwent drastic fluctuations. In 1965, the lake levels were near their historic lowstand, rebounding to near their historic highstand in the mid 1980s, and approaching the lowstand again in the present. These fluctuations are documented by hydrographs produced by USGS gauging stations. Figure 3.1 displays hydrograph information taken from station 10010000 near Saltair harbor, which is located about 5 km from the study site, in which lake surface elevations are plotted against time. Analysis of the aerial images of the study site capture channel morphology adjustments, including full channel avulsions, over the range of historic lake levels.

Figure 3.2 displays the images of Lee Creek over the time series of this study. This stream appears to have undergone a period of major incision between 1965 and the present. Between 1965 and 1997, the lower portion of the stream did not have an incised channel; instead this reach was characterized by broad sheetflow. As lake levels

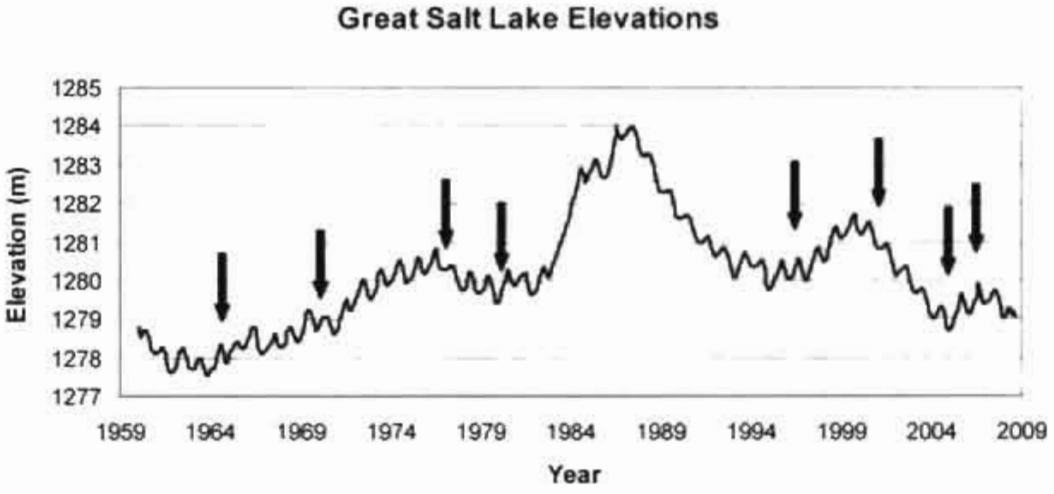

Figure 3.1. Great Salt Lake hydrograph for USGS station 1001000. Arrows indicate the years for which aerial images of the study site were found.

Figure 3.2. Aerial images of the Lee Creek from 1965 to 2006. Images from 2001 and 2005 are VNIR 1,2,3 N band 15 m resolution satellite images available from the Intermountain Region Digital Image Archive Center (IRDIAC). All other images are aerial photographs available from the Utah Automated Geographic Reference Center (AGRC). With the exception of the 2006 image, a 1-foot resolution color image, they are 1-m resolution black and white images.

1965

1971

1977

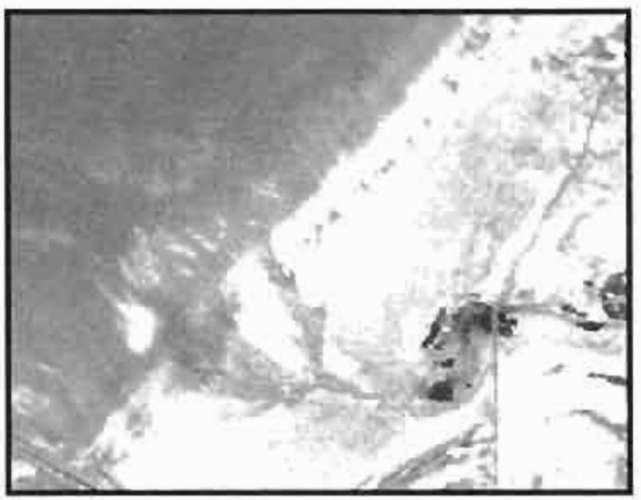

1980

N

1 km

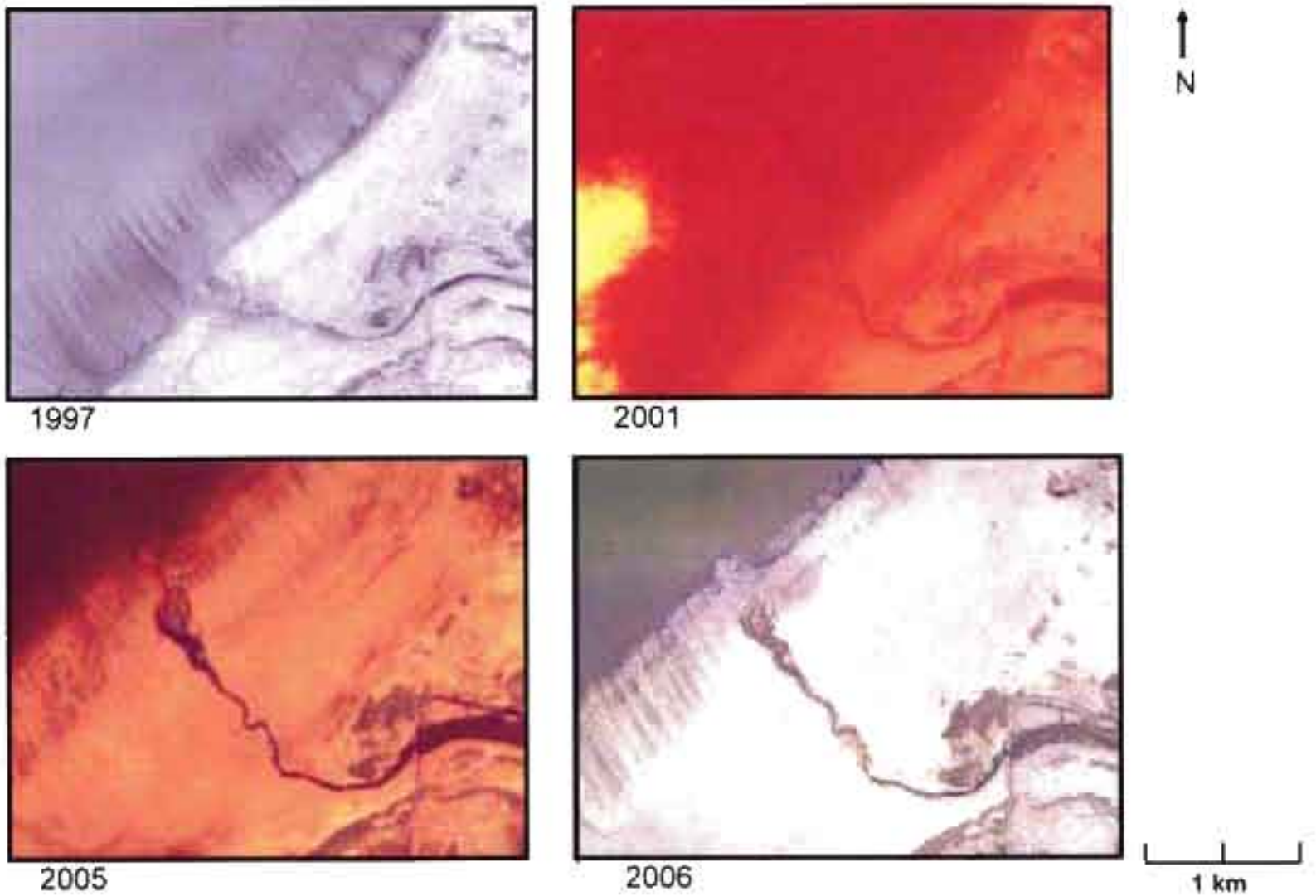
1997
2001
N
2005
2006
1 km

regressed between 1997 and the present, the creek was able to form a fully incised channel. This is recognizable in aerial images by the transition from sheetflow to a single channel thread. A shift of a short distal reach of the channel takes place between September 2005 and October 2006 in the delta area. Otherwise, the newly incised channel appears to be relatively stable.

Figure 3.3 displays the aerial images series of the Goggin Drain. By comparison, this stream has been more avulsive over the same time period. Between 1965 and the present, the Goggin underwent three major and several smaller avulsions, and four periods of incision. For the purpose of this study, major avulsions are defined to be full avulsions of nearly the entire natural channel, in which incised channels that deviate from the main channels are observed. Such events are documented in the 1977, 1997 and 2005 images.

The 1965 and 1971 images show the Goggin Drain as lake levels were near their historic lowstand of ~1278 m. Between 1971 and 1977, lake levels rose by about 3m. During this time, the Goggin Drain underwent a complete avulsion, with flow shifting from the west to the north. Lake levels continued to rise, and in 1983, the study site was completely submerged, and remained underwater until 1989. Between 1989 and 1997, as the lake regressed, the main stream channel did not reoccupy its former channel, but shifted to the southwest, appearing to breach a portion of the canal in the process, and forming the delta observed in the 1997 image. A period of incision followed, as the 2001 image shows the evolution of a single threaded, more sinuous channel. Between 2001 and 2005, lake levels regressed by about 2.5 m, lengthening the channel to the west. During this time, avulsions took place, with smaller channels diverging from several points along

Figure 3.3. Aerial images of the Goggin Drain from 1965 to 2006. Images from 2001 and 2005 are VNIR 1,2,3 N band 15 m resolution satellite images available from the Intermountain Region Digital Image Archive Center (IRDIAC). All other images are aerial photographs available from the Utah Automated Geographic Reference Center (AGRC). With the exception of the 2006 image, a 1-foot resolution color image, they are 1-m resolution black and white images.

1965

1971

N

1977 – Avulsion 1

1980

1 km

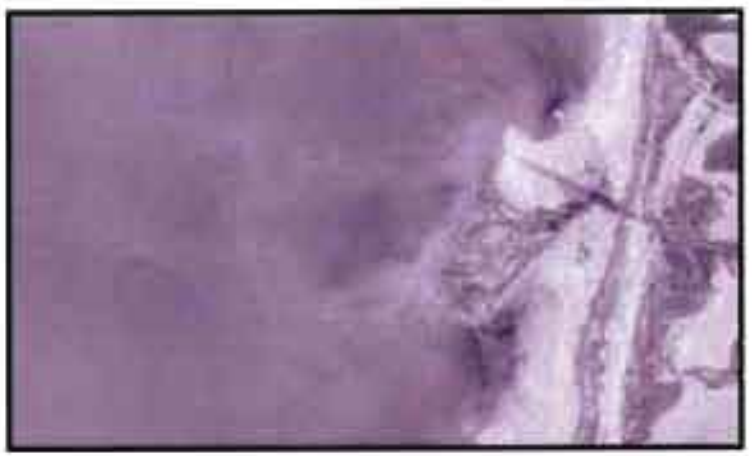

1997 – Avulsion 2

2001

N

2005 – Avulsion 3

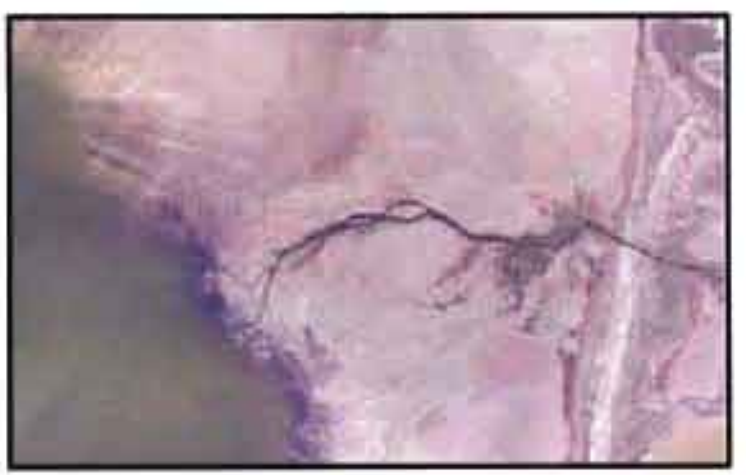

2006

1 km

the main channel. Although flow did not completely shift to these channels, this behavior is interpreted as an avulsion, as the channels produced are well defined with some incision. Field investigations in 2008 showed these channels to be active during times of high discharge. The modern channel form has remained relatively unchanged since 2006.

After each period of major avulsion, incision follows (1977 to 1980, 1997 to 2001, 2005 to present), which is displayed in the aerial images by the transition from sheetflow to single channel threads. The 1980 and 2006 images show distributary channels forming downstream of incised areas, which are interpreted as minor avulsions of small portions of the channel, typical of deltaic systems.

For both streams, some data has been lost to the high lake levels in the mid 1980s. The LiDAR image of the field area (Figure 3.4) recreates the water level at the 1986 highstand, with dry land displayed in orange and water displayed in blue, and shows the field area completely submerged at this time.

Avulsion Chronology

Figure 3.5 shows the Great Salt Lake hydrograph with the timing of channel avulsions of the Goggin Drain marked. Brackets indicate the time period in which each of the avulsions took place based on inferences drawn from the available aerial images.

Hydrograph Analysis

Stream hydrographs plotting discharge over time for both the Lee Creek and Goggin Drain were analyzed in order to investigate how discharge patterns may related to channel morphology. Stream hydrographs also provide information on the occurrence of

Figure 3.4. ArcGIS image of the field site during the 1986 Great Salt Lake highstand. Orange shades represent dry land, blue represents submerged land. The lake level at this time was 1284 m.

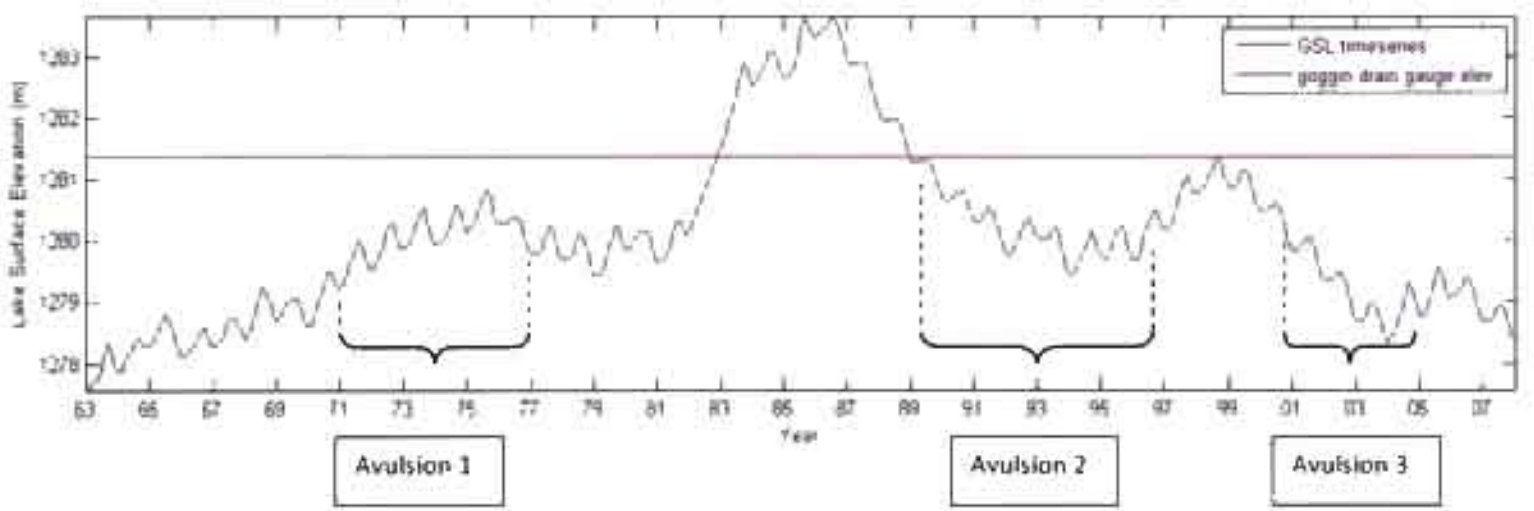

Figure 3.5. Great Salt Lake hydrograph indicating bracketed timeframes for avulsion events. The horizontal line demarks the elevation of the Goggin Drain hydrograph, and for lake levels above this line, the entire study site was submerged.

flooding and how it may relate to the timing of channel avulsions. For the time period extending from the 1980s to the early 2000s, no data are available because high lake levels inundated the sites. Therefore the discharge information is shown for the periods prior to the lake highstand, and following the regression (Figures 3.6 and 3.7). Note that the Lee Creek measurements were was discontinued by the USGS in April of 2008. Figures 3.8 and 3.9 show the available discharge data displayed as multiples of base flow, a technique for visually interpreting the variability of discharge in each stream.

To assist in determining potential avulsion triggers for the Goggin Drain, the hydrograph for the Jordan River Surplus Canal was investigated for use as a proxy for the missing data for this stream. For each year in which data for both systems was available, discharge for the peak flooding months was correlated (see Appendix A), and an almost perfect linear relationship was found, suggesting that the Surplus Canal data could be used as a proxy for the Goggin Drain. Figure 3.10 displays the hydrographs of both streams. Figure 3.11 compares the stream hydrographs to the lake hydrograph, with avulsion periods marked.

Modern Fluvial Geomorphology

Descriptive LiDAR Analysis

The high-resolution LiDAR images display many sedimentary structures and geomorphic features that are not visible in aerial photographs, as well as some features that are not visible in the field. ArcMap images readily display these features, including some of the features observed in the time series of aerial images. Figure 3.12 shows the entire field site in a grayscale LiDAR DEM. A more detailed image of the Goggin Drain (Figure 3.13) displays several remnant channels surrounding the main stream channel.

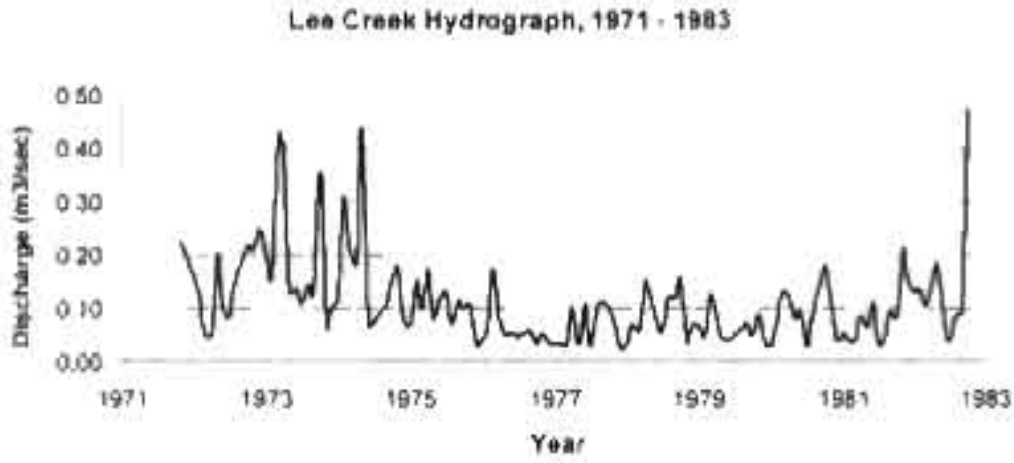

(A)

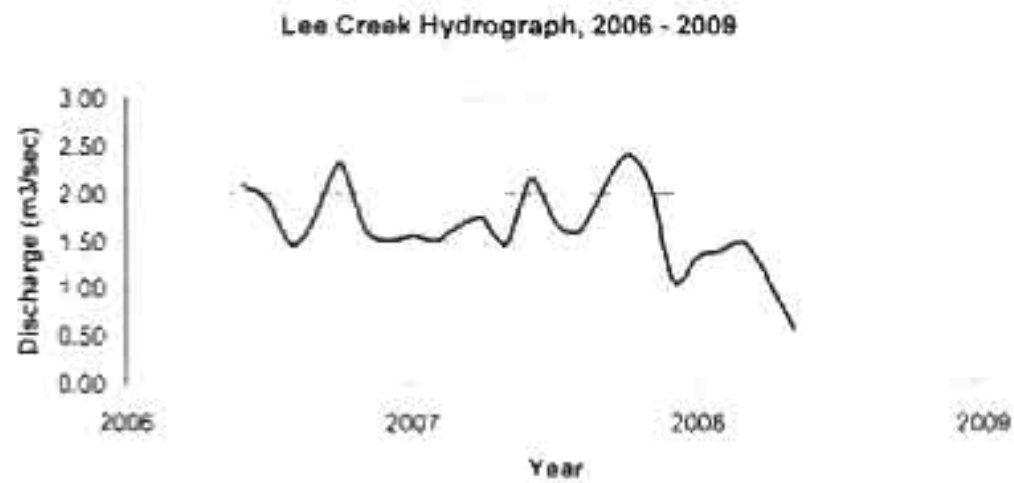

(B)

Figure 1.6 Lee Creek hydrographs.

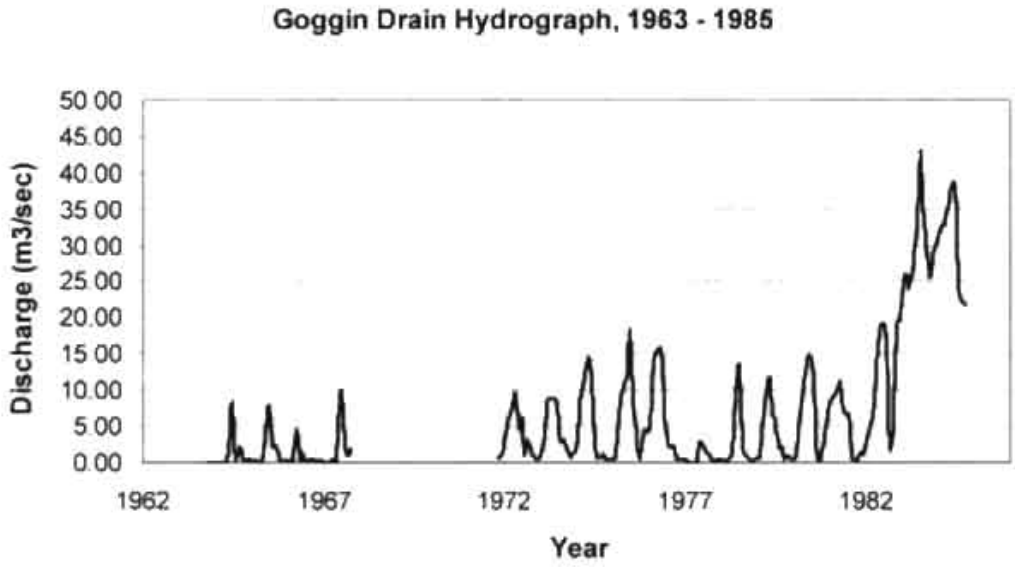

(A)

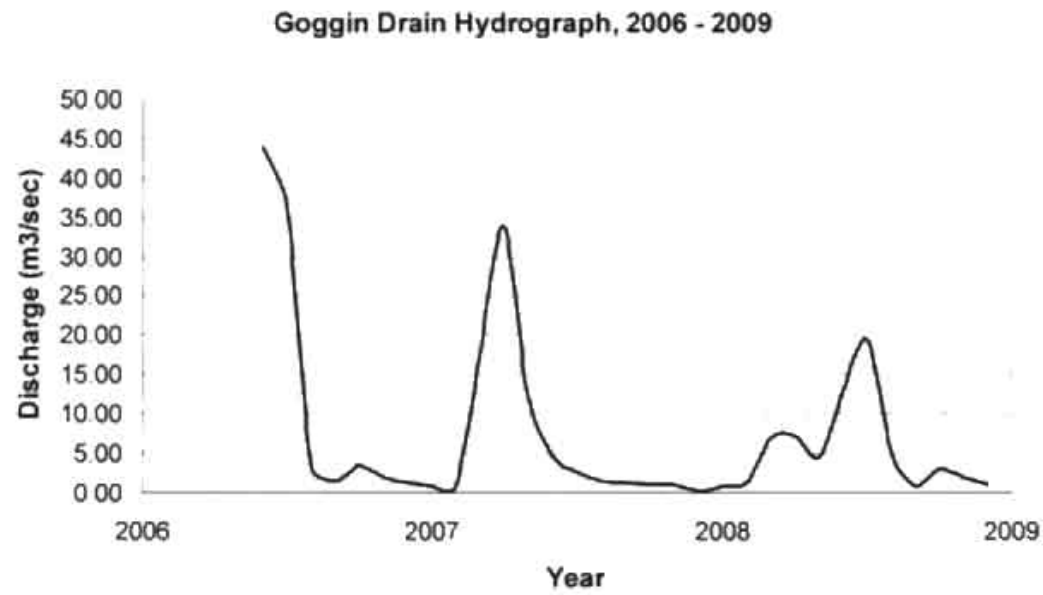

(B)

Figure 3.7. Goggin Drain hydrographs.

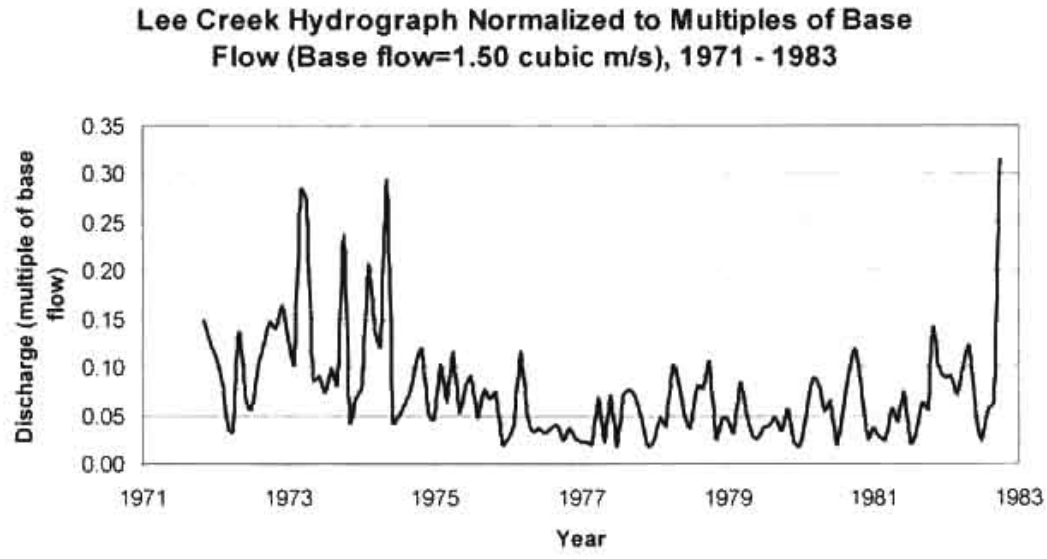

(A)

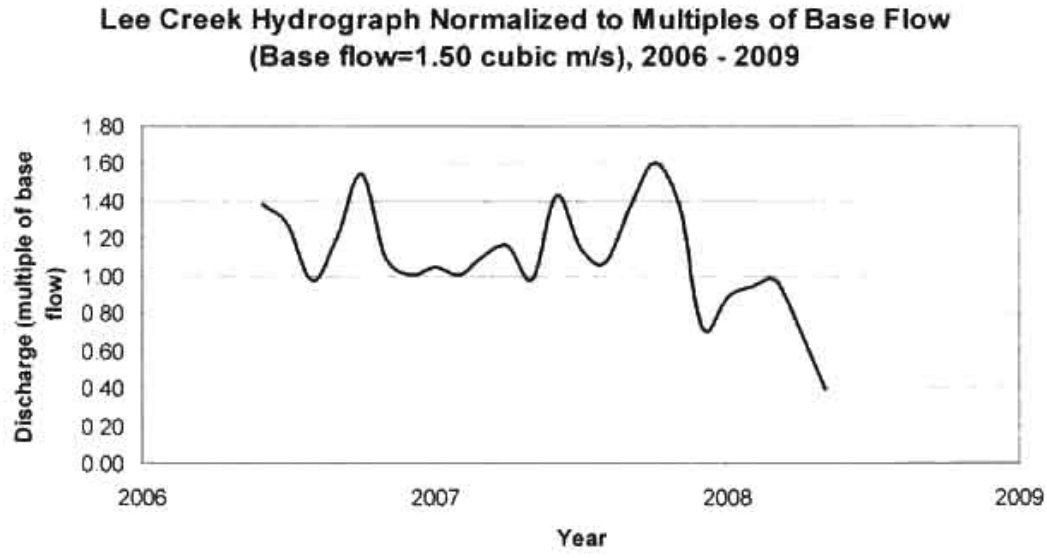

(B)

Figure 3.8. Lee Creek hydrographs normalized to multiples of base flow.

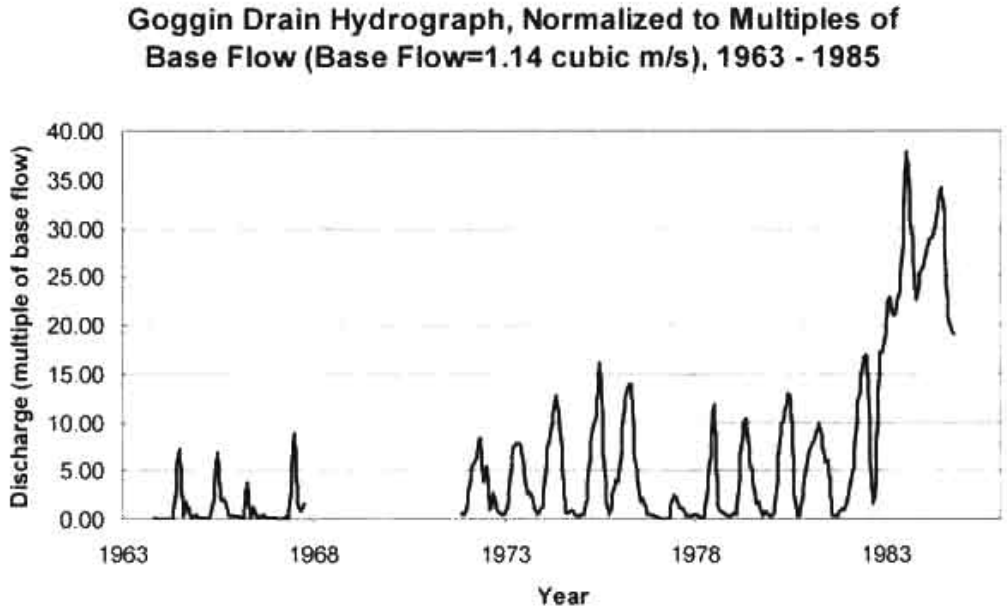

A)

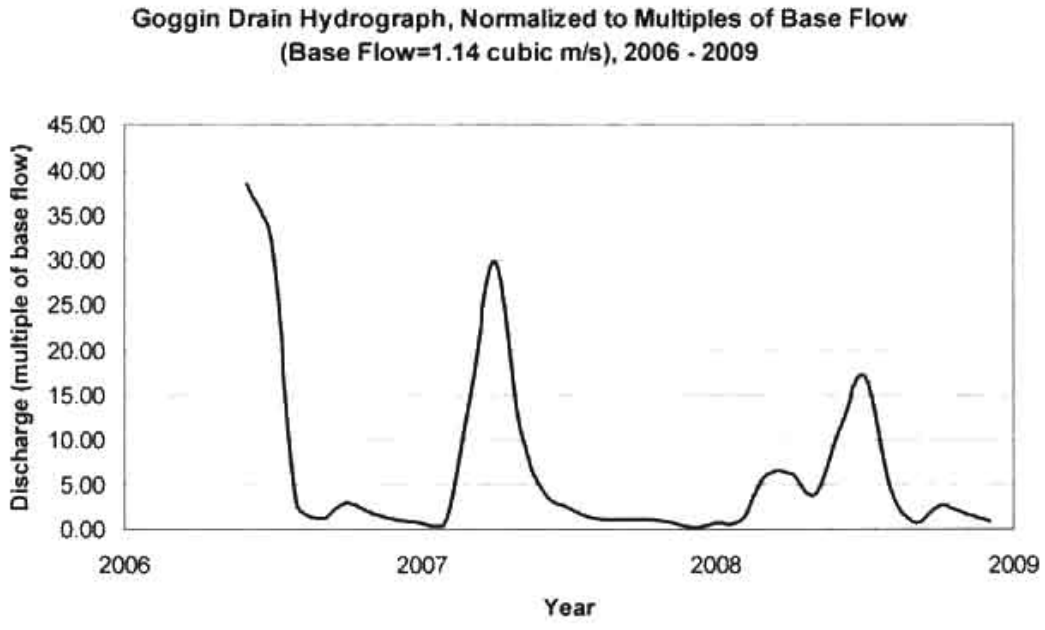

(B)

Figure 3.9. Goggin Drain hydrographs normalized to multiples of base flow.

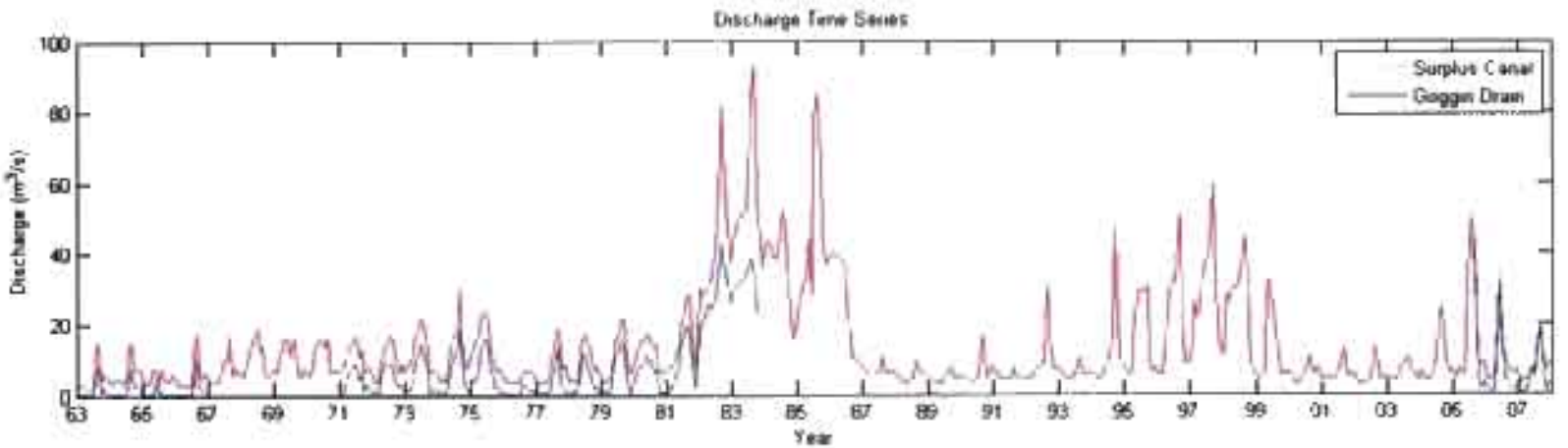

Figure 3.10. Hydrographs of the Goggin Drain and the Jordan River Surplus Canal.

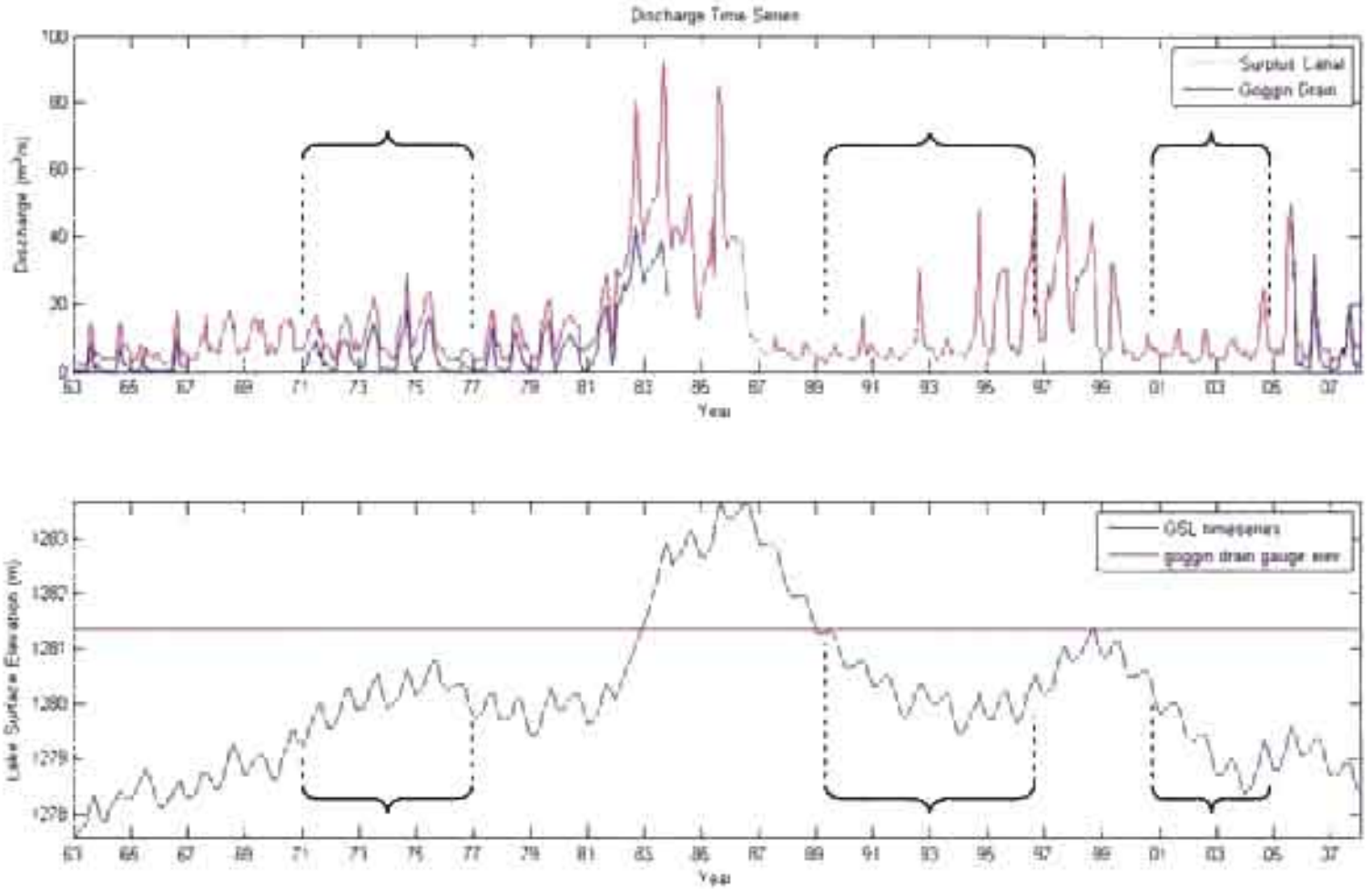

Figure 3.11. Stream Hydrographs and Great Salt Lake Hydrograph with Goggin Drain avulsion periods bracketed.

Figure 3.12. Grayscale 1.25 m gridded LiDAR image of the field site.

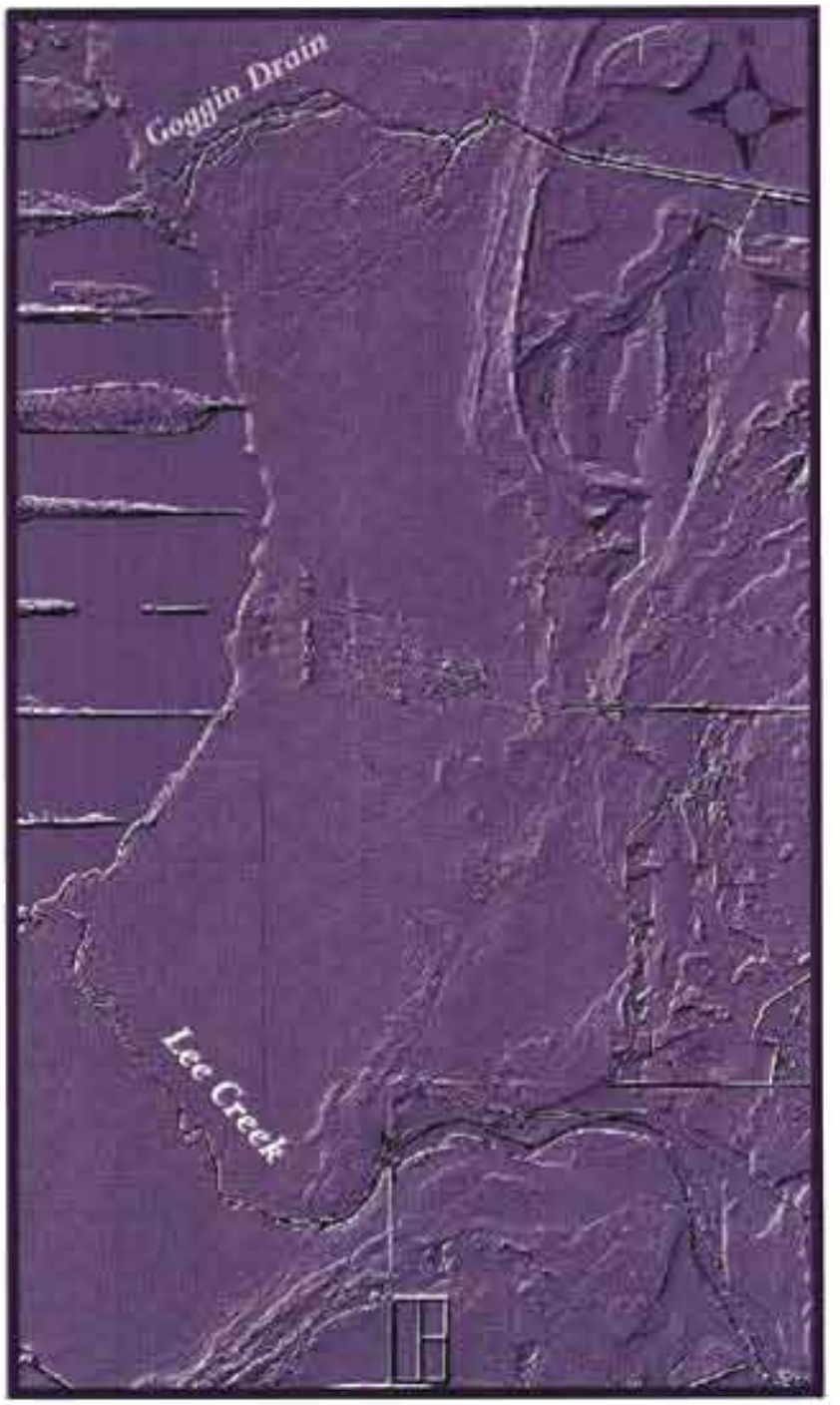

1 km

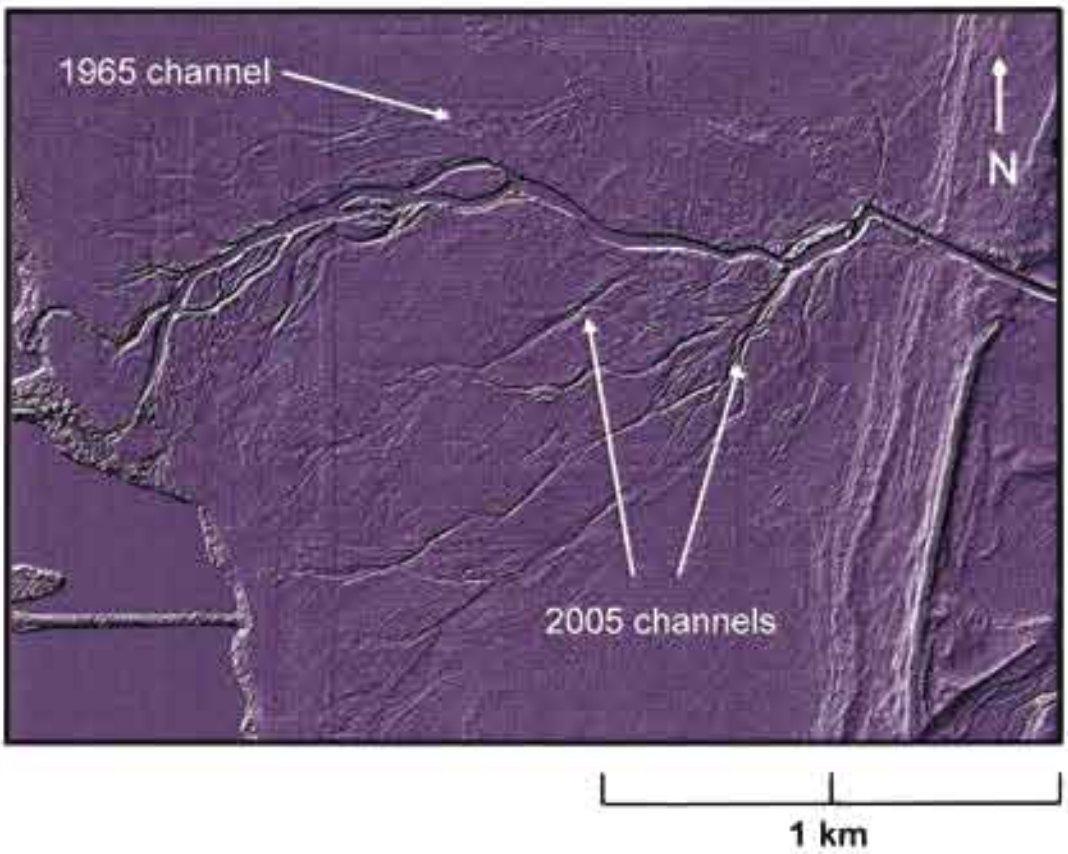

Figure 3.13. Grayscale LiDAR image of the Goggin Drain showing several remnant channels.

Comparison to the aerial images shows the large remnant channel north of the modern channel that was the main flow path observed from 1965 to 1971 (Figure 3.3). This channel was abandoned in the avulsion observed between 1971 and 1977. The remnant channels south of the modern channel can be linked to the 2005 avulsion, after which many active channels developed to the south. These channels were abandoned during the period of incision that followed.

A color-ramped image (Figure 3.14) at the transition of the canal to the natural channel shows a remnant highstand delta that is not readily visible in the field or in aerial images. This delta can be seen forming in the 1997 aerial photograph (Figure 3.3). Lake levels were relatively high at this time, and as they regressed between 1997 and the present, this delta was abandoned.

The images of the Lee Creek reflect a system that has been less dynamic. The channel morphology has remained relatively consistent over time and does not show remnant channels and avulsion paths similar to those seen surrounding the Goggin, although some potential crevasse splays are evident (Figures 3.15 and 3.16). In these images, there is no evidence of remnant deltas.

Modern Features

Other low relief sedimentary structures revealed in color-ramped images include erosional rills, crevasse splays and beach ridges. These features are displayed in Figures 3.17 -3.19. Figures 3.20 and 3.21 show the airborne LiDAR images overlain with the DEM produced in the terrestrial LiDAR survey of the Goggin Drain. The detail displayed by LiDAR provided useful quantitative geomorphic data used in modeling velocity within the channels.

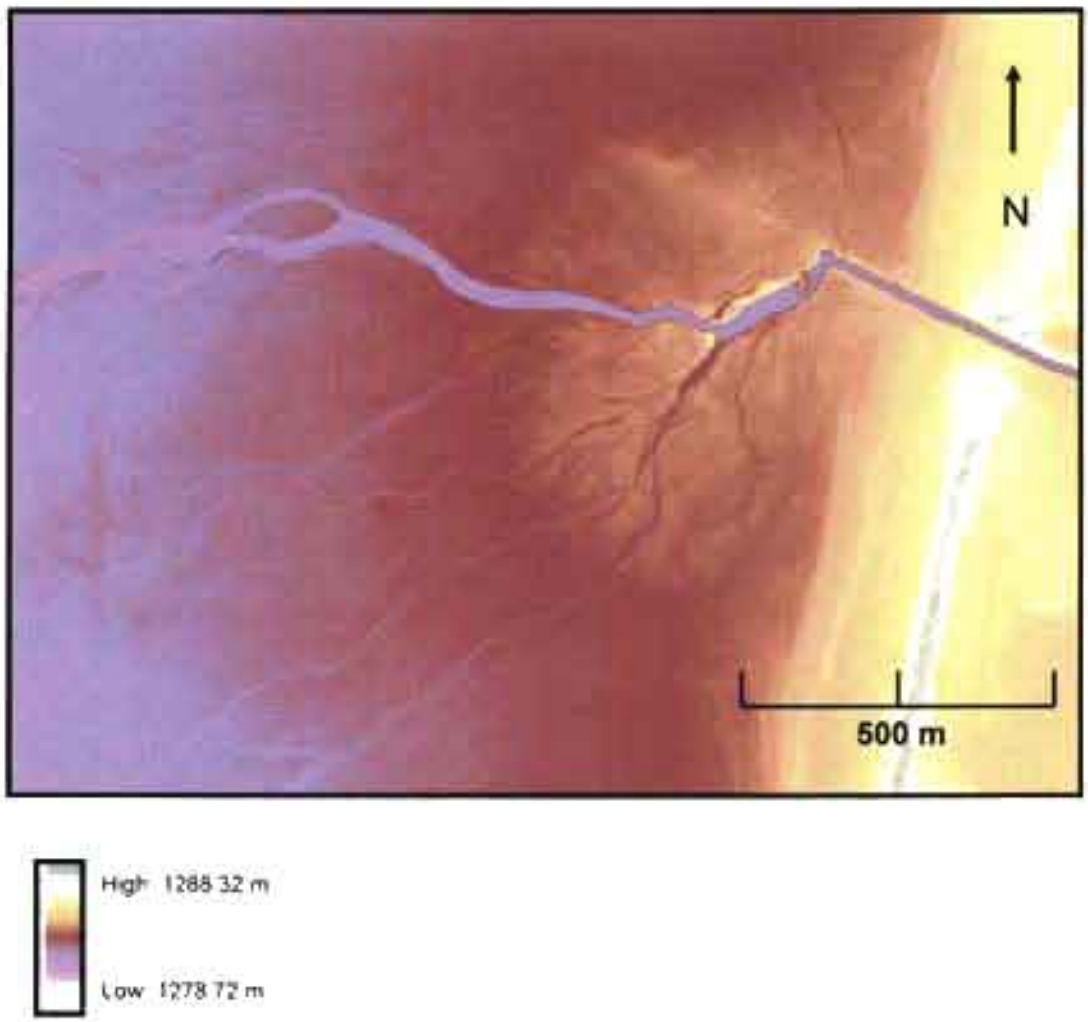

Figure 3.14. A color-ramped image of the Goggin Drain displays a highstand delta surrounding transition point between the natural channel and the canal.

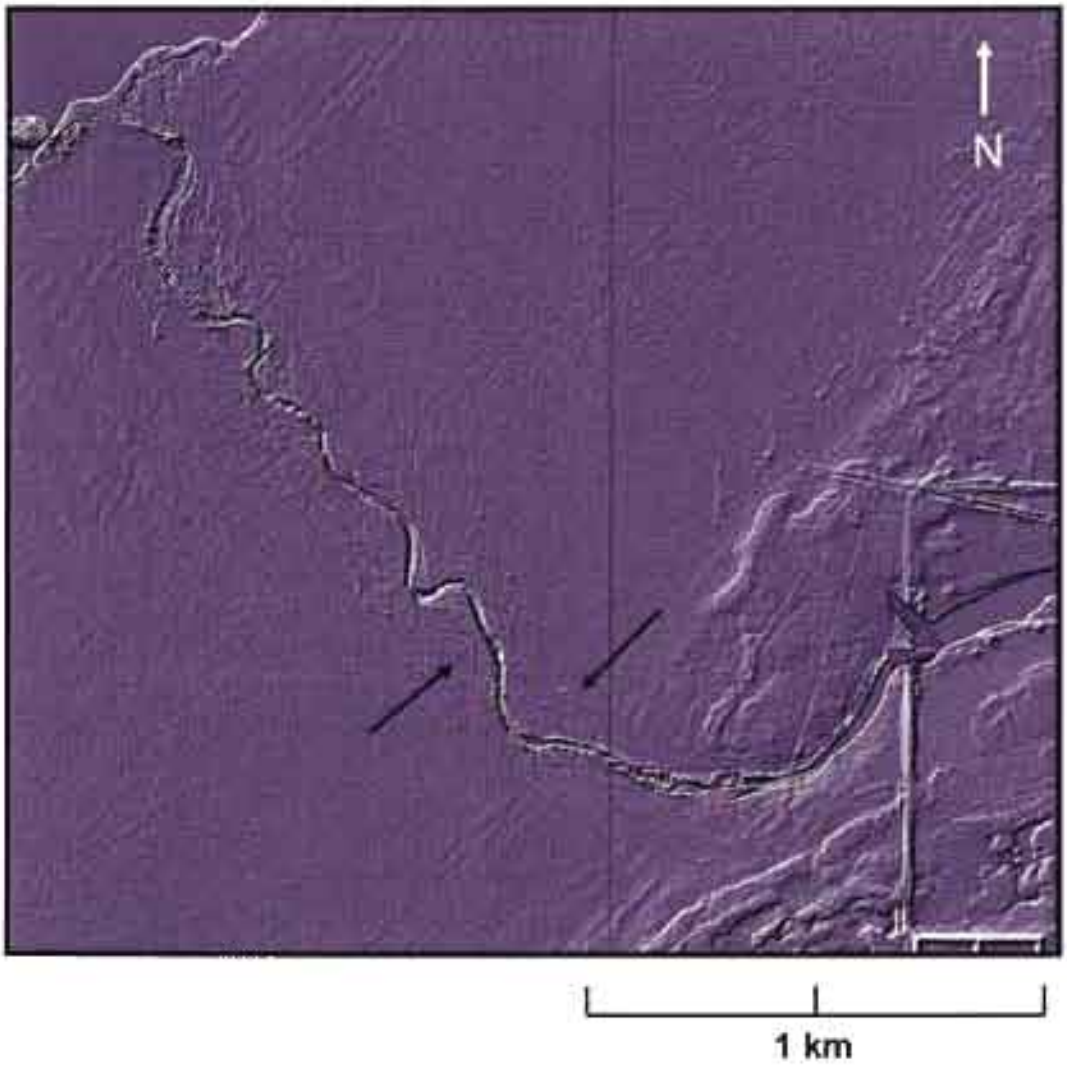

Figure 3.15. Grayscale airborne LiDAR image of the Lee Creek. Note that while some small crevasse splays are visible (marked with arrows), no significant remnant channels are present.

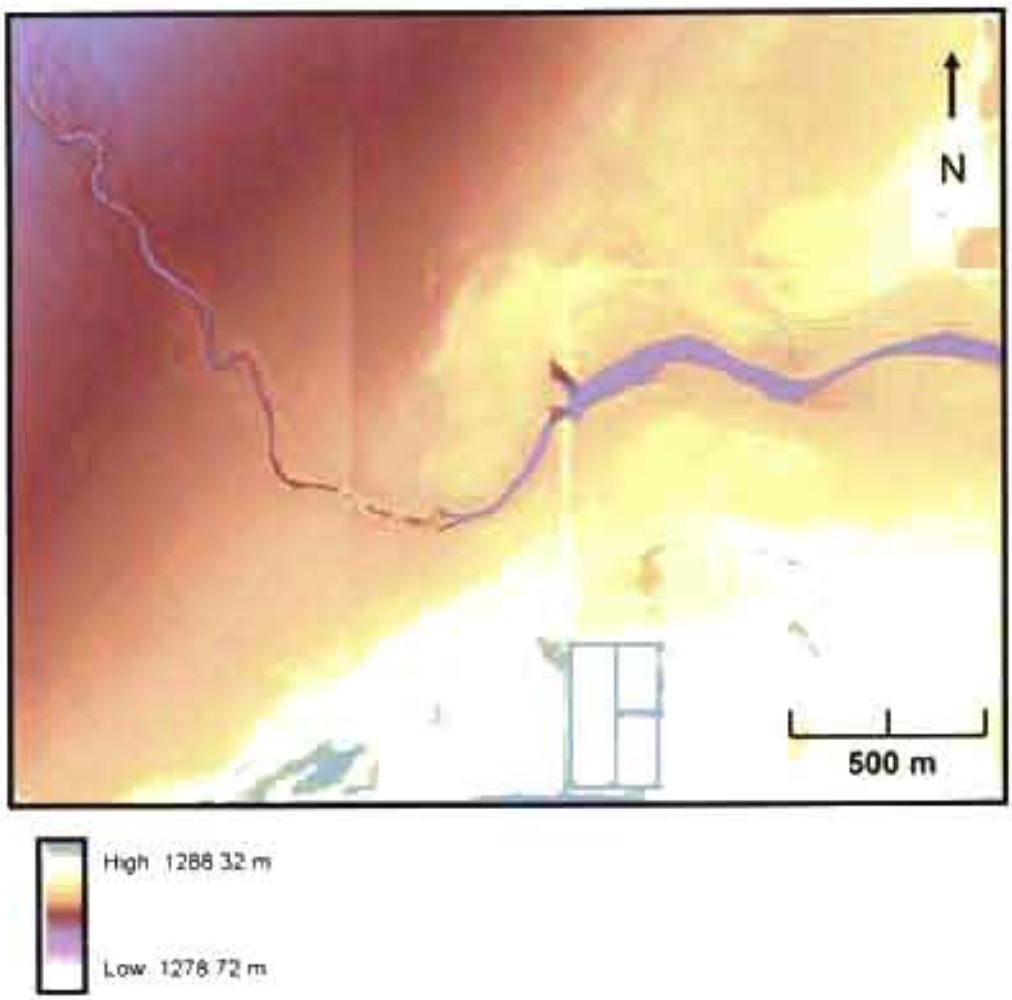

Figure 3.16. A color-ramped airborne LiDAR image of the Lee Creek. It does not show evidence of highstand deltas as seen near the Goggin Drain.

Figure 3.17. Beach ridges surrounding the Lee Creek.

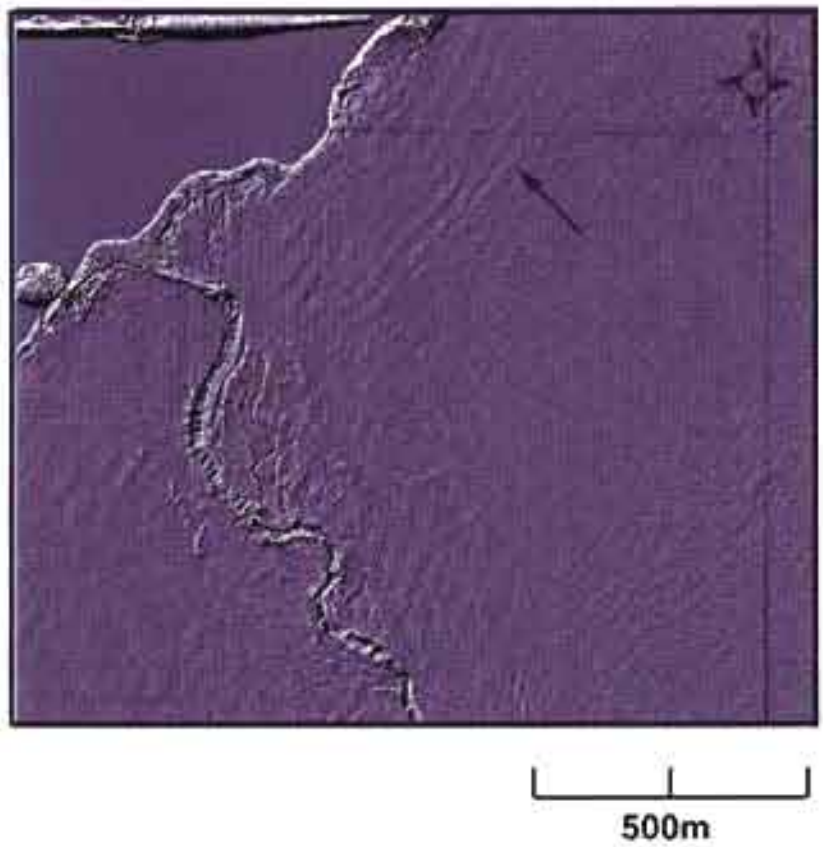

Figure 3.18. More beach ridges surrounding the Lee Creek.

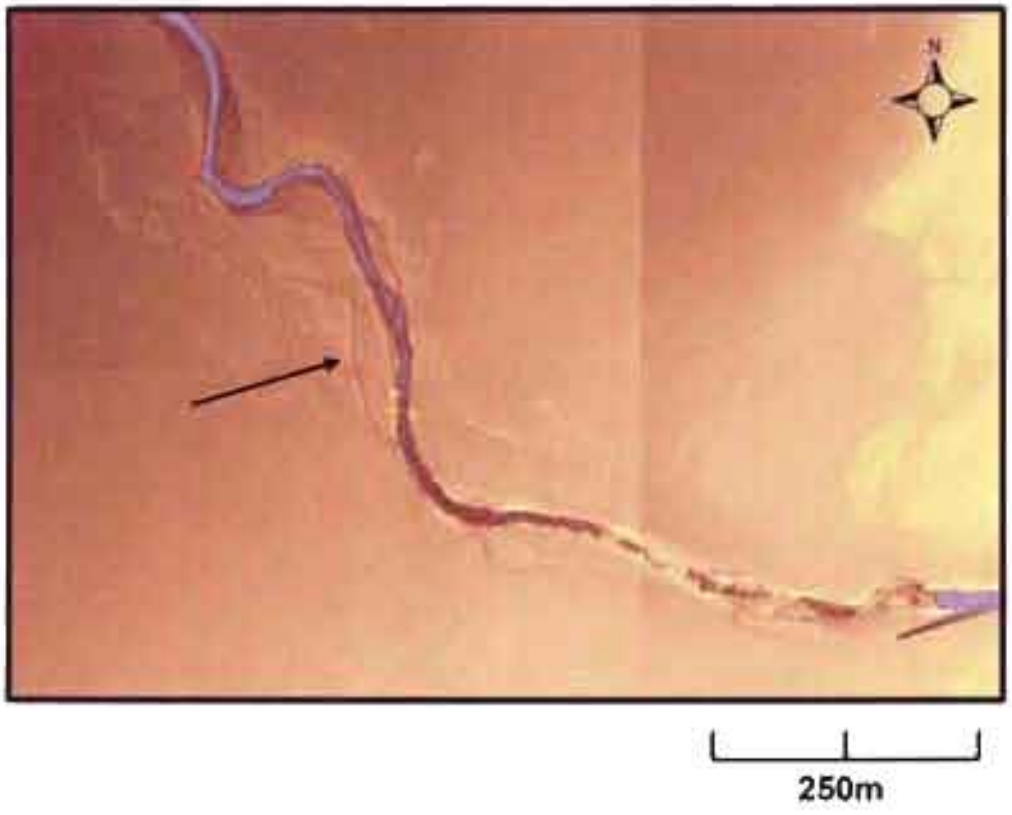

Figure 3.19. Airborne LiDAR image of incised rills and crevasse splays surrounding the Lee Creek.

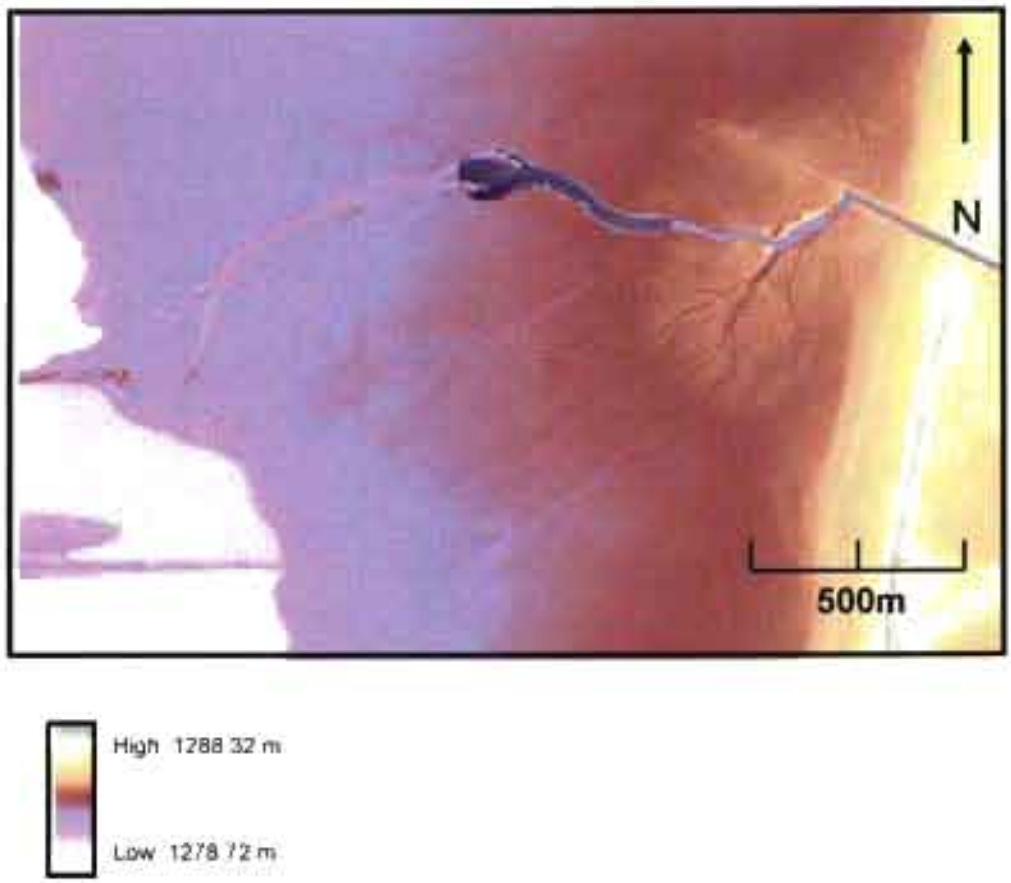

Figure 3.20. Large scale airborne LiDAR image of the Goggin Drain overlain with terrestrial imagery.

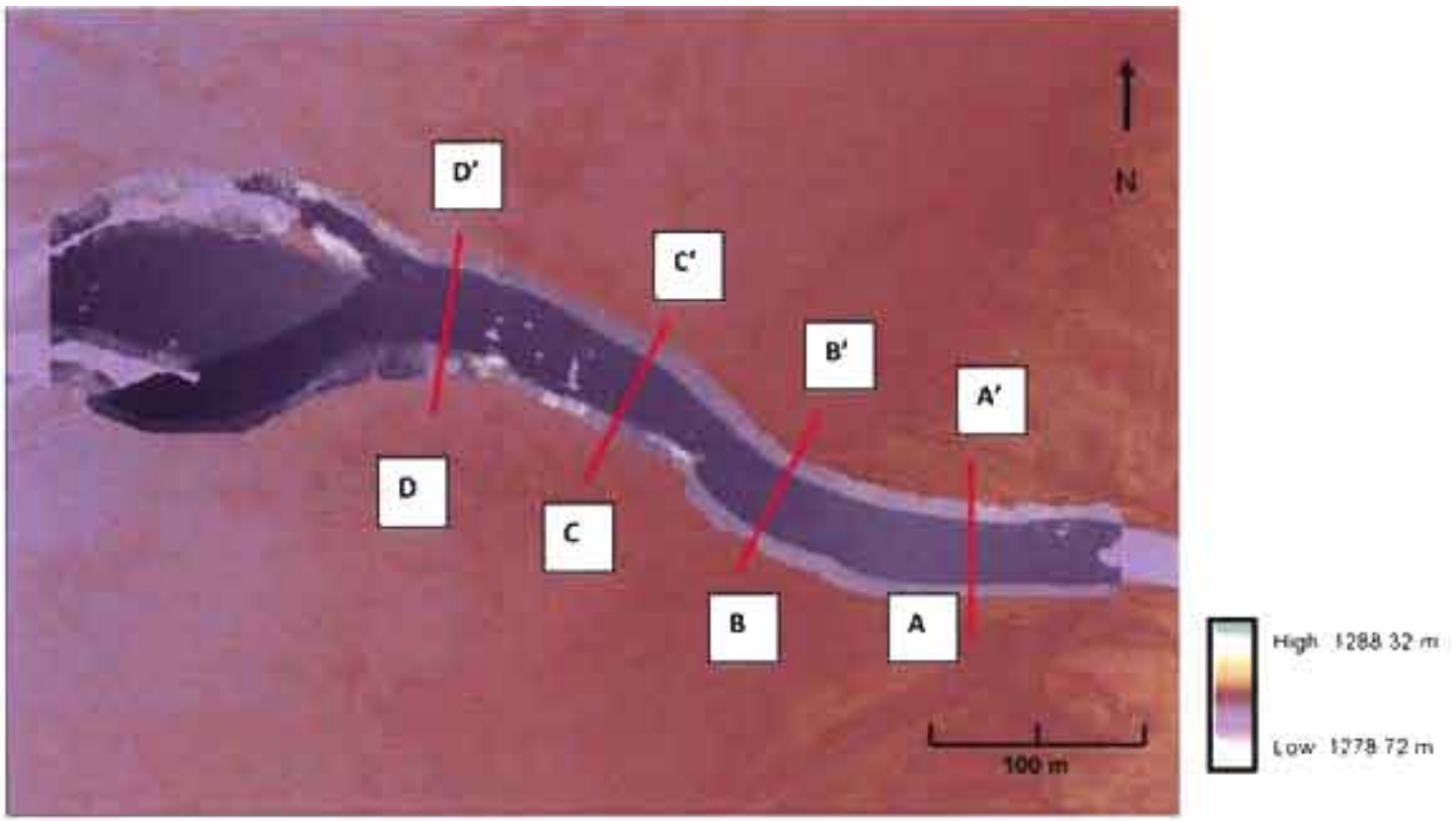

Figure 3.21. Terrestrial LiDAR image of the Goggin Drain. Red lines indicate the location of cross sections shown in Figure 3.29.

Channel Characterization

From a combination of DEM analysis and field measurements, data were collected for the purpose of describing the channel morphology of the Lee Creek and the Goggin Drain. Points along the stream were designated as measurement waypoints, each representing the most headward point of a short reach with internally similar geomorphic conditions. Channel measurements of width, incision depth and water depth were taken at these points. The raw data, including the exact geographic location of each waypoint measurement, is displayed in Appendix B: Channel Morphology Data. Sinuosity was calculated using distance measurements from the airborne LiDAR data; stream length was divided by valley length. These geomorphic data have been summarized in Tables 3.1 and 3.2. Based on the field and LiDAR data collection, three geomorphic reaches were defined for each stream, each having fairly consistent width, incision, sinuosity and vegetation cover. Channel measurement data from individual waypoints within these reaches has been averaged. Reaches are pictured in Figures 3.22 through 3.25.

LiDAR Longitudinal and Cross-Sectional Profiles

Longitudinal profiles of the streams were created based on the airborne LiDAR images. Figures 3.26 and 3.27 shows these profiles along with the elevation of the bank alongside the channel, effectively displaying the variation in channel incision along the profile. The degree of incision captured by the profiles corresponds to field observations; the Lee Creek is most incised in the middle reach (reach 2), and the Goggin Drain is most incised in the upper reach (reach 1). The water surface profile was used to derive the gradient at each waypoint and the average gradient within each reach for use in velocity calculations. It is assumed that the steep gradients at the lakeshore in these profiles are

Table 3.1: Geomorphic attributes of Lee Creek

Reach	Description of channel form	Average Width (m)	Average total incision (m)	Gradient (m/m)	Sinuosity	Vegetation Cover (%)
1	Broad shallow channel with smooth low angle banks which are covered thickly with vegetation. Incision is very slight.	14.1	0.76	1.42E-03	1.16	50
2	Channel becomes narrow and deeply incised. Two nickpoints are found in this section. Banks are generally rough and nearly vertical, with multiple erosional terraces present in some reaches. Rough channel bottom alternates between pools and resistant caliche-lined runs. Remnant channels and short, deep erosional rills flank the stream.	5.1	2.03	1.36E-03	1.20	25
3	As incision decreases, the channel takes the form of a distributary delta. Sandbars are present, and incision and vegetation cover are reduced.	12.3	0.79	4.50E-04	1.23	0-10

Table 3.2. Geomorphic attributes of the Goggin Drain.

Reach	Description of channel form	Average Width (m)	Average incision to channel bed (m)	Gradient (m/m)	Sinuosity	Vegetation Cover (%)
1	The stream is released from its canal and flows as a single-threaded channel down the highstand delta. Many dry remnant channels surround the main flow path.	29.1	1.15	4.83E-04	1.11	50
2	Incision decreases, and banks are near vertical and highly eroded. The main channel disperses into two to three segments with large islands in between them. Resistant caliche layers line the channel bed.	32.7	0.81	7.70E-04	1.08	30
3	Here the stream forms a broad distributary delta. Incision depths are small and vegetation cover is negligible.	35.4	0.46	6.26E-04	1.06	<5

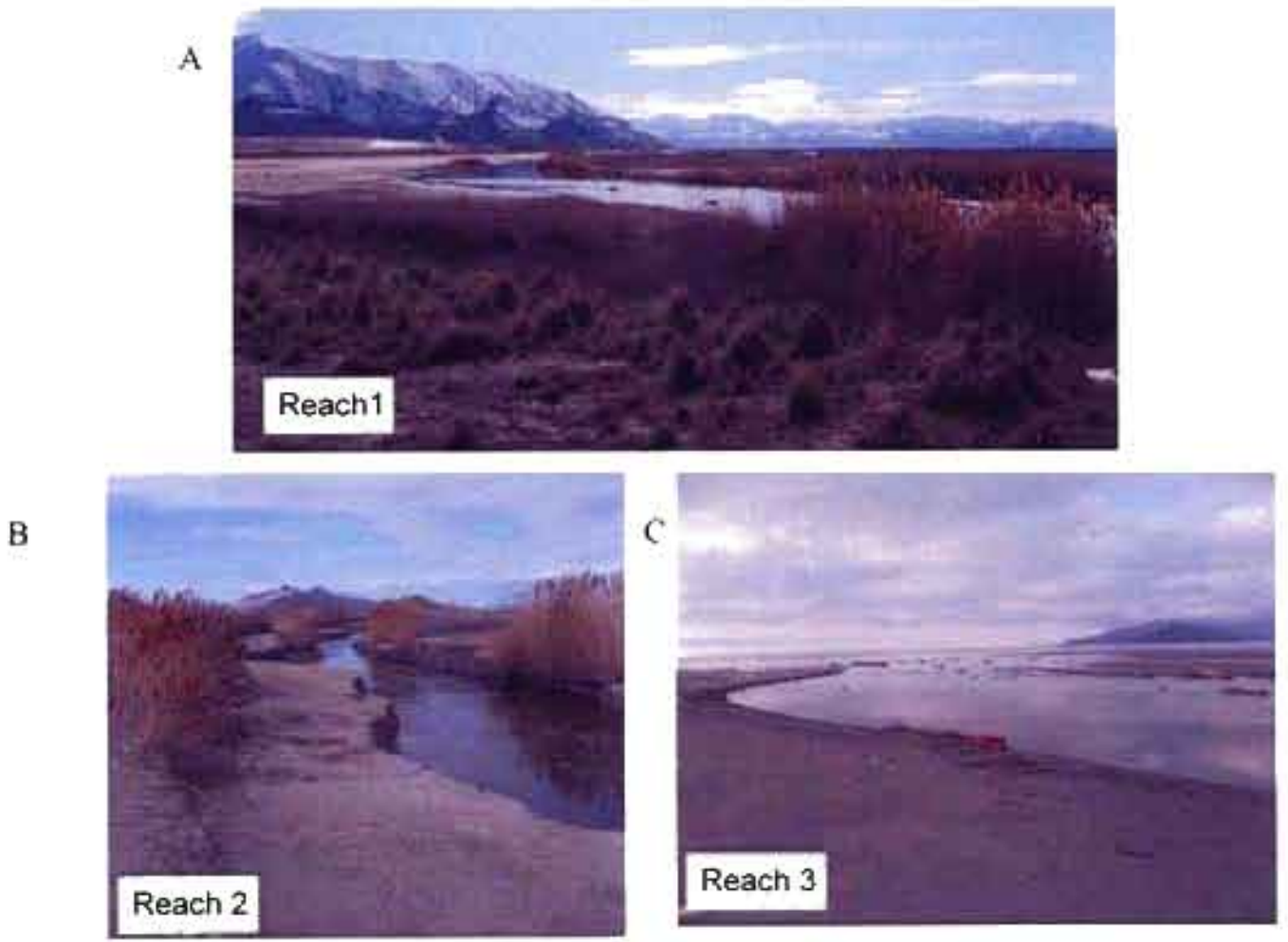

Figure 3.22. Field photographs of Lee Creek.

Figure 3.23. Field photograph of reach 1 of the Goggin Drain.

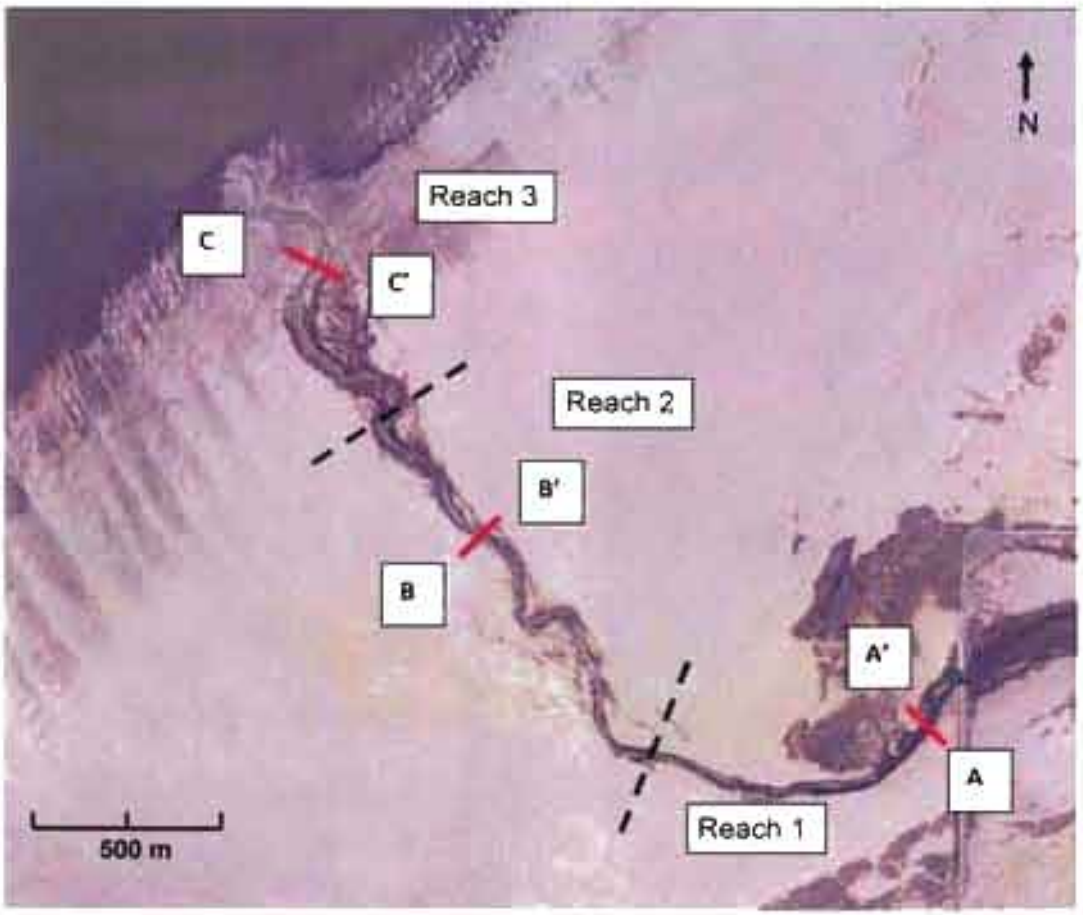

Figure 3.24. Aerial photograph of the Lee Creek with three geomorphically distinct reaches designated. Dashed black lines indicate the boundaries of each reach, and solid red lines indicate the location of cross sectional profiles taken from the airborne LiDAR DEMs.

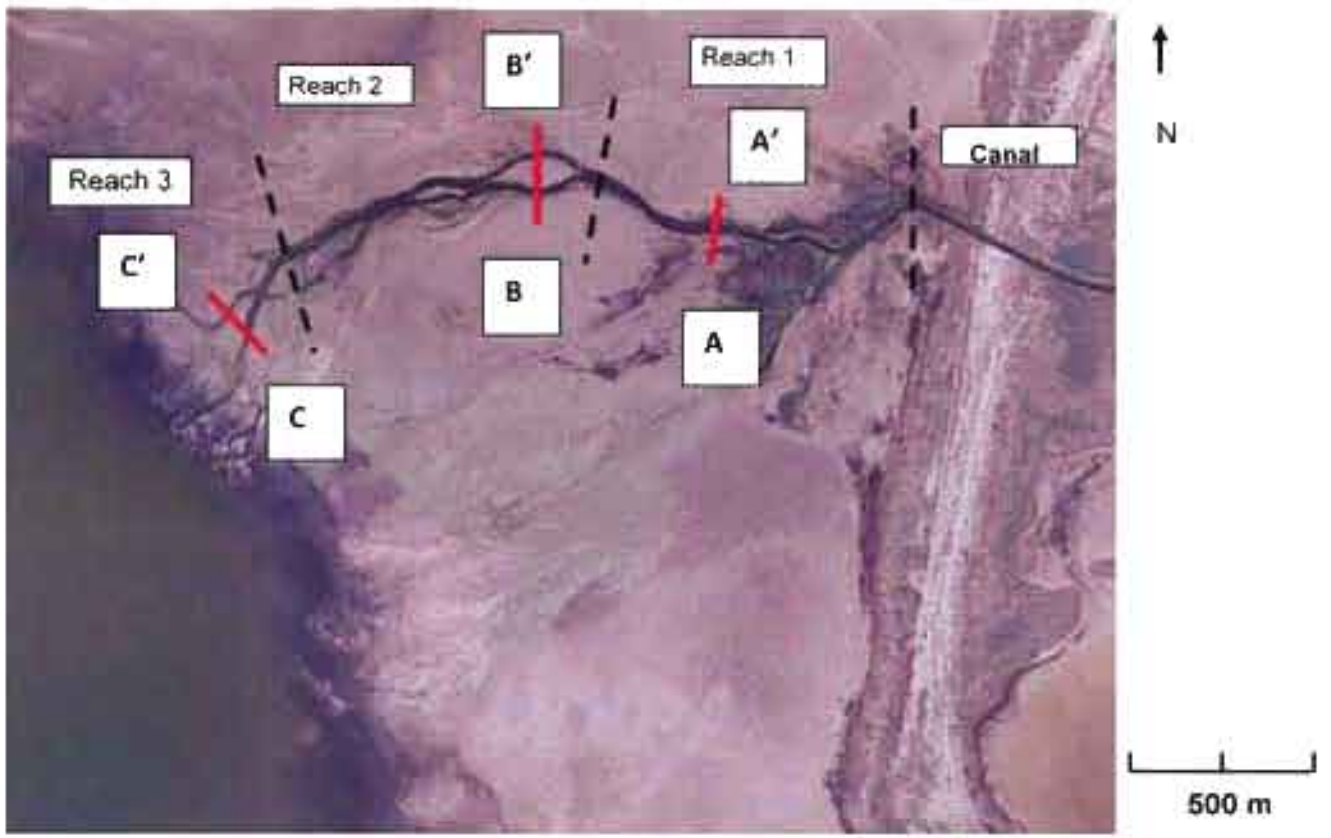

Figure 3.25. Aerial photograph of the Goggin Drain with three geomorphically distinct reaches designated. Dashed black lines indicate the boundaries of each reach, and solid red lines indicate the location of cross sectional profiles taken from the airborne LiDAR DEMs.

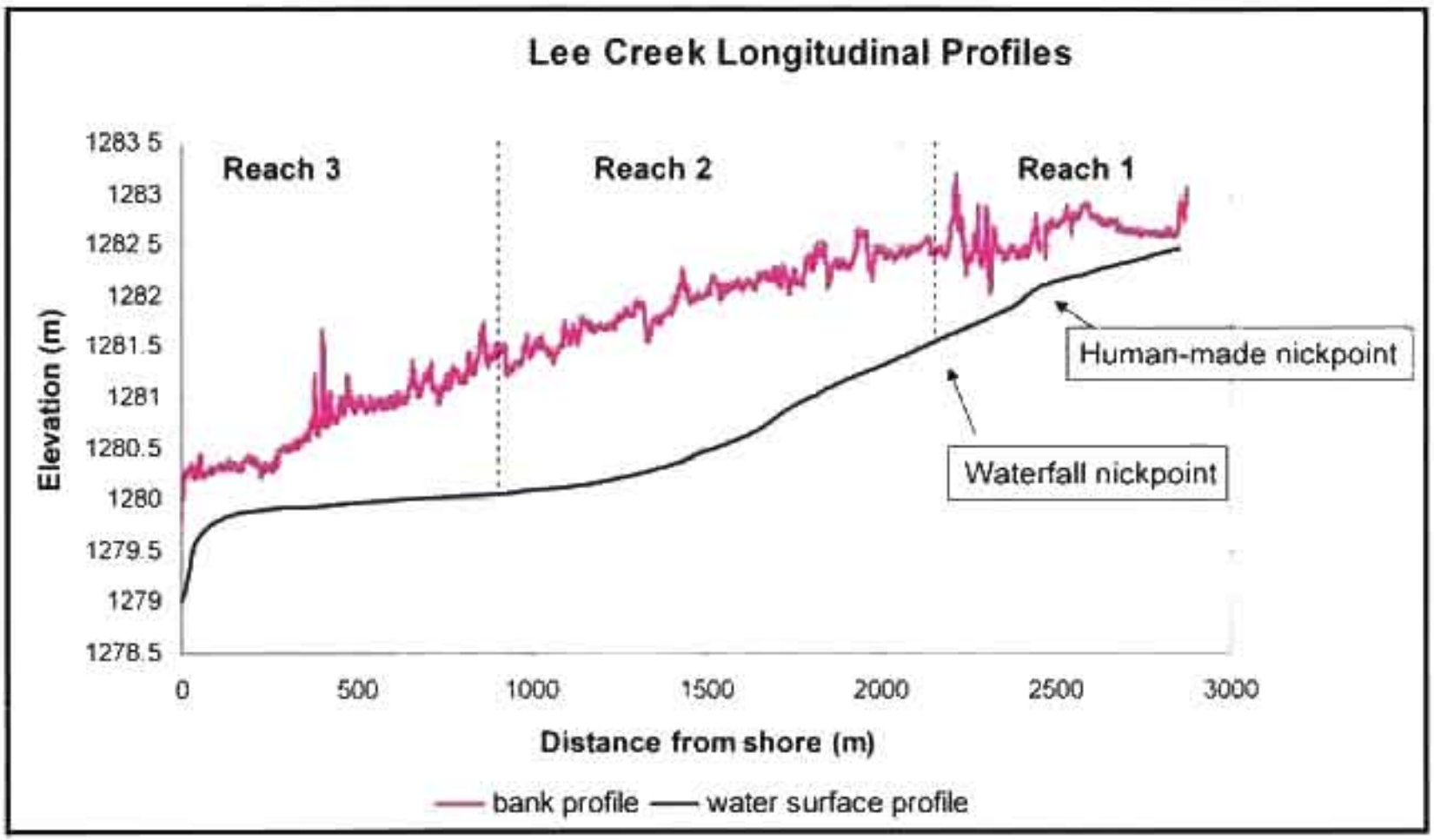

Figure 3.26. Longitudinal profile of the Lee Creek.

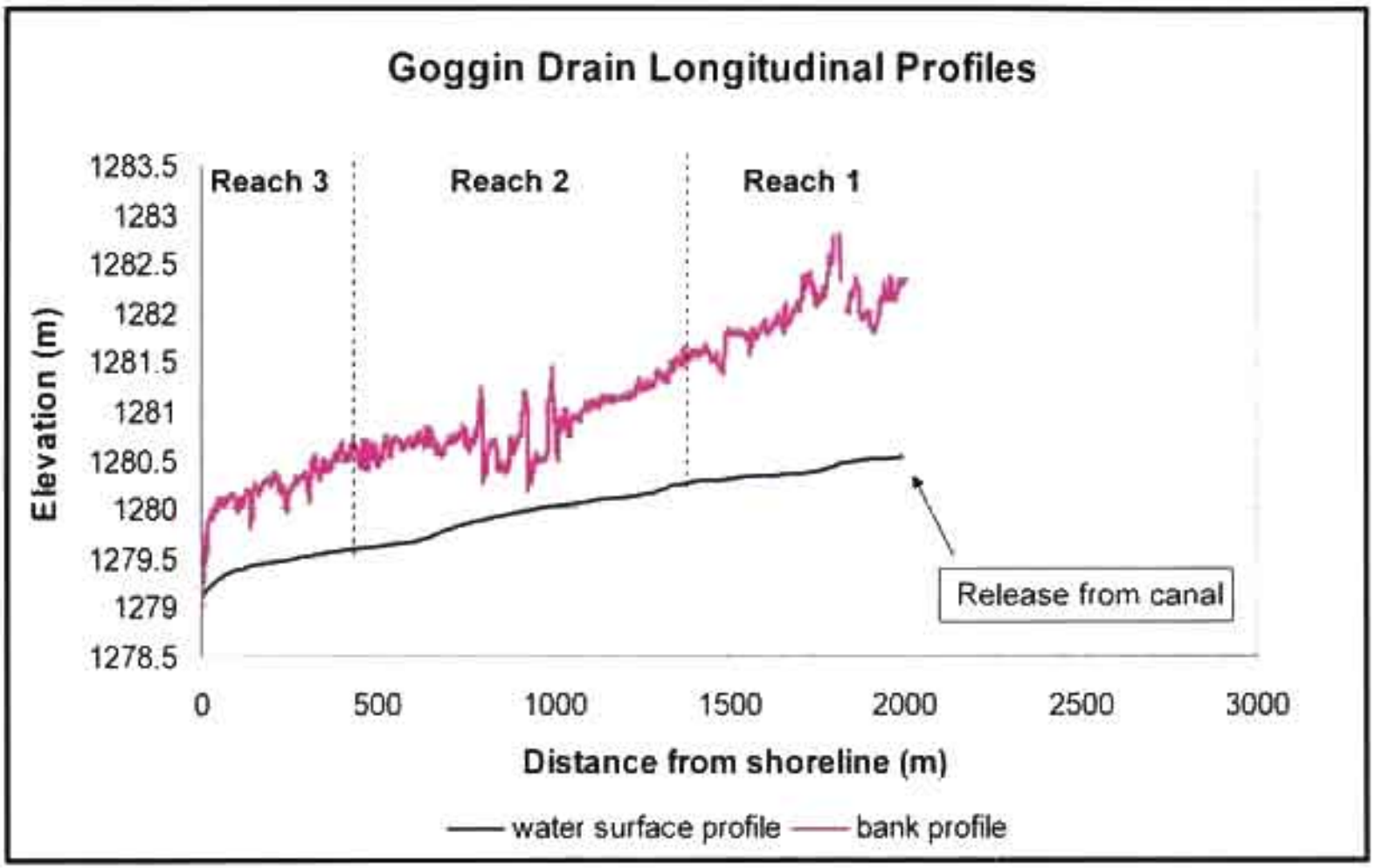

Figure 3.27. Longitudinal profile of the Goggin Drain.

produced by errors due to gaps in data over the lake surface; these steeper gradients are not observed in the field.

Cross sections of each reach produced from aerial LiDAR data are displayed below (Figures 3.28 and 3.29). When the airborne LiDAR survey was flown, the channels contained water, so these profiles display the fluvial incision to the water surface. The ground-based LiDAR survey was conducted when the Goggin Drain was nearly dry, so the degree of incision to the channel bed is displayed in these profiles (Figure 3.30). Note the prominent levees displayed in many of the profiles, especially in the Goggin Drain (Figure 3.30). The degree of incision captured by these profiles is consistent with what is observed in the field and in the longitudinal profiles; the greatest incision in the Lee Creek is observed in Reach 2, while incision in the Goggin Drain remains more constant.

The volume of sediment removed by incision was calculated for each channel by using the incision depth and surface area for each waypoint along the channel. The total volume removed at the Lee Creek was 3.46×10^5 m^3 and the total volume removed at the Goggin Drain was 5.55×10^5 m^3. Complete tables showing the volume calculations for each reach may be found in Appendix C.

Modern Channel Hydraulics

Calculation of Velocity

For each geomorphic reach of the Lee Creek, the average cross-sectional velocity was calculated. For the initial calculations, velocities are representative of the discharge in which water depth measurements were made, which was $0.88 m^3/s$. Velocities were then calculated over the range of discharges seen according to the USGS hydrograph.

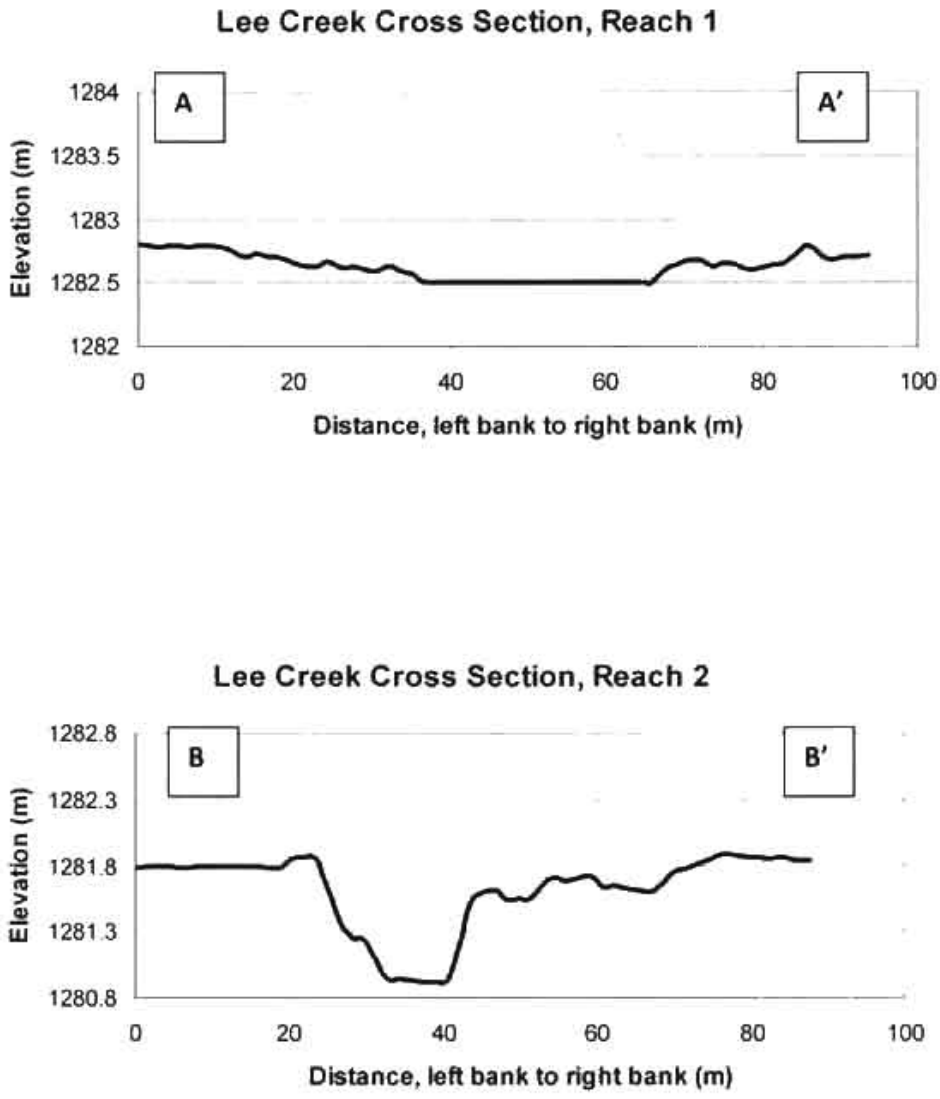

Figure 3.28. Cross-sectional profiles of the Lee Creek produced from airborne LiDAR.

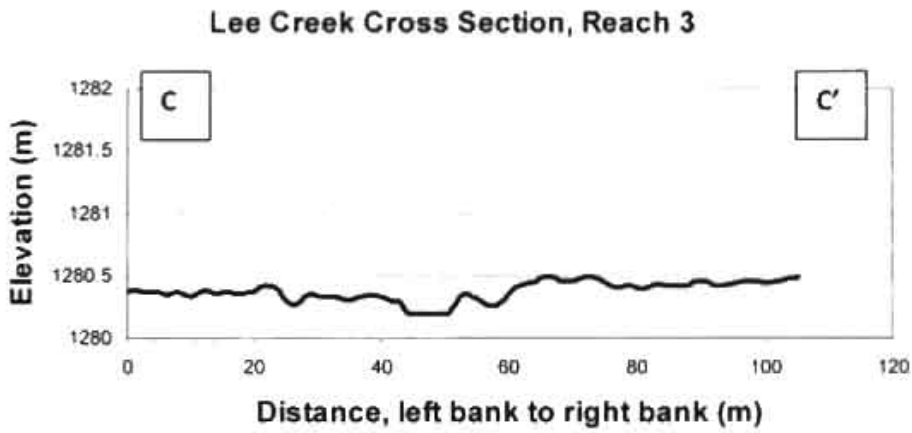

Figure 3.28 continued.

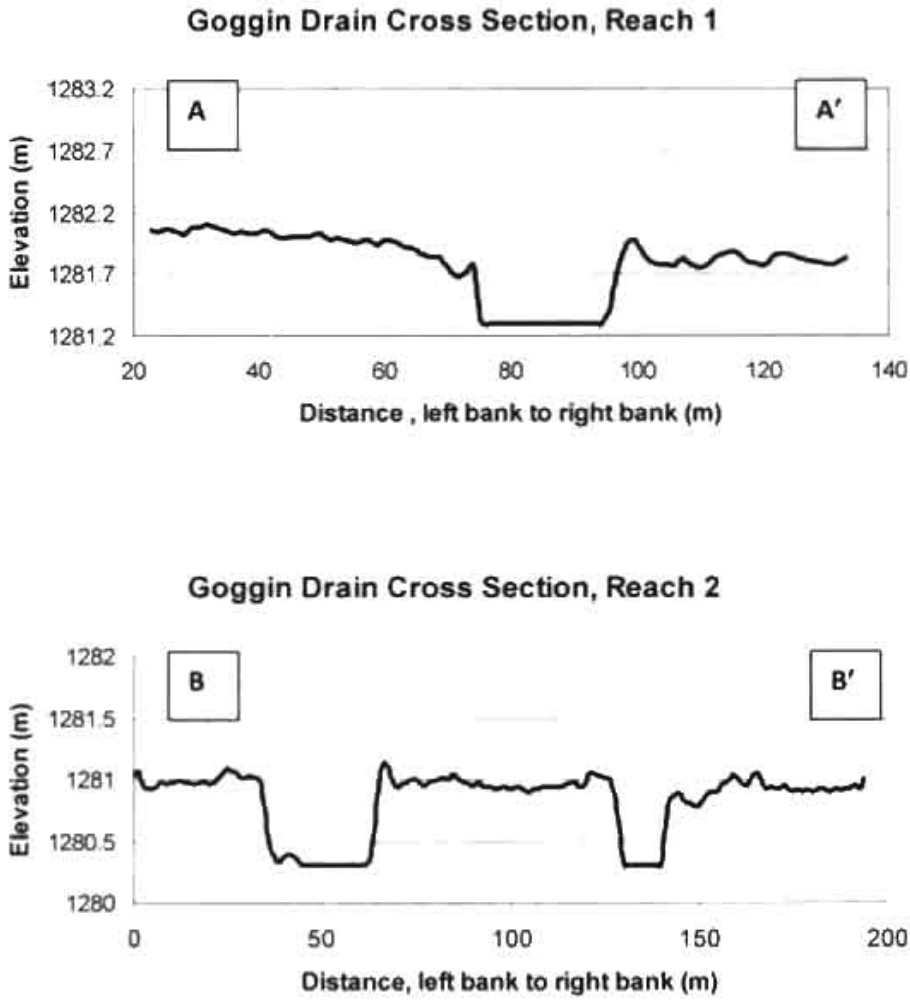

Figure 3.29: Cross-sectional profiles of the Goggin Drain produced from airborne LiDAR.

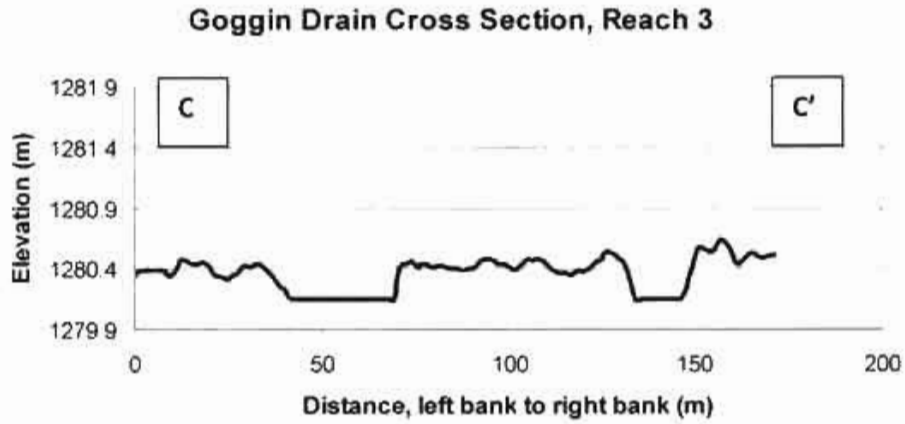

Figure 3.29 continued

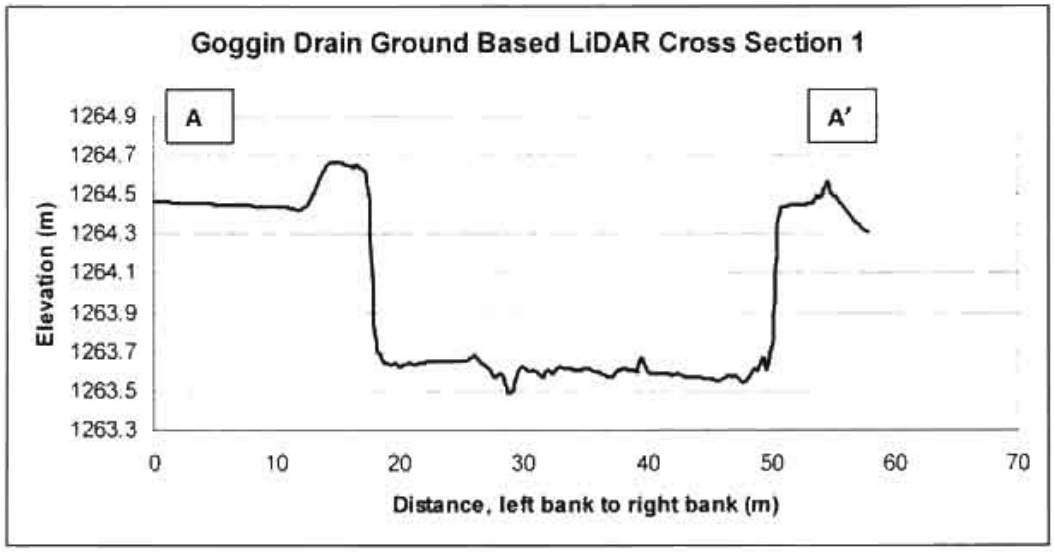

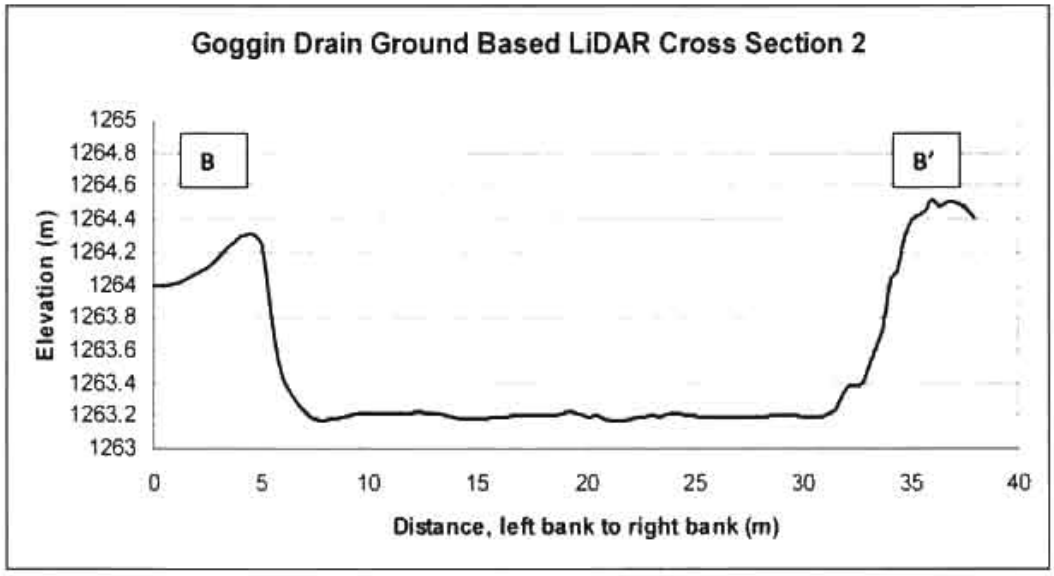

Figure 3.30. Goggin Drain cross-sectional profiles produced from terrestrial LiDAR.

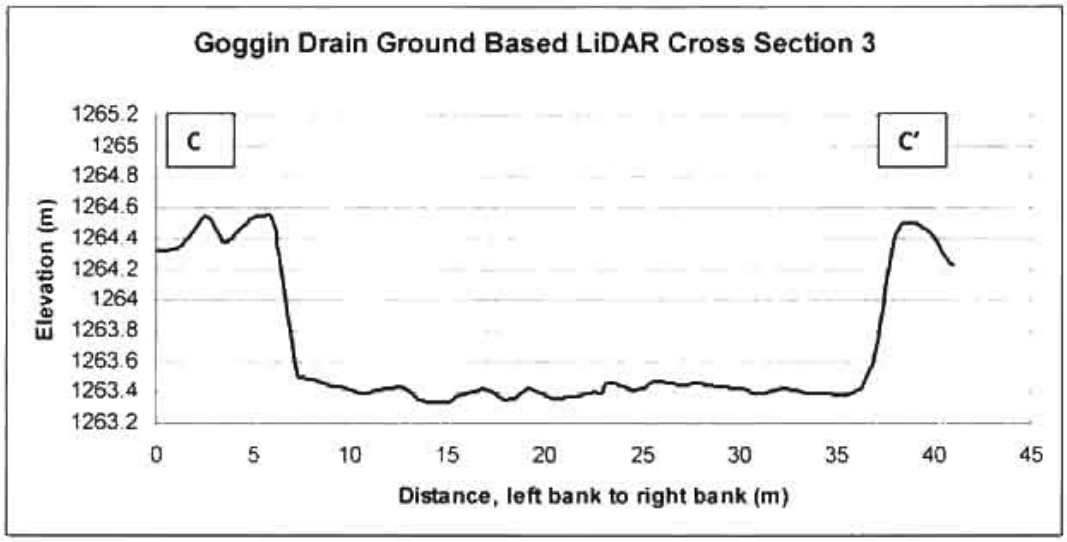

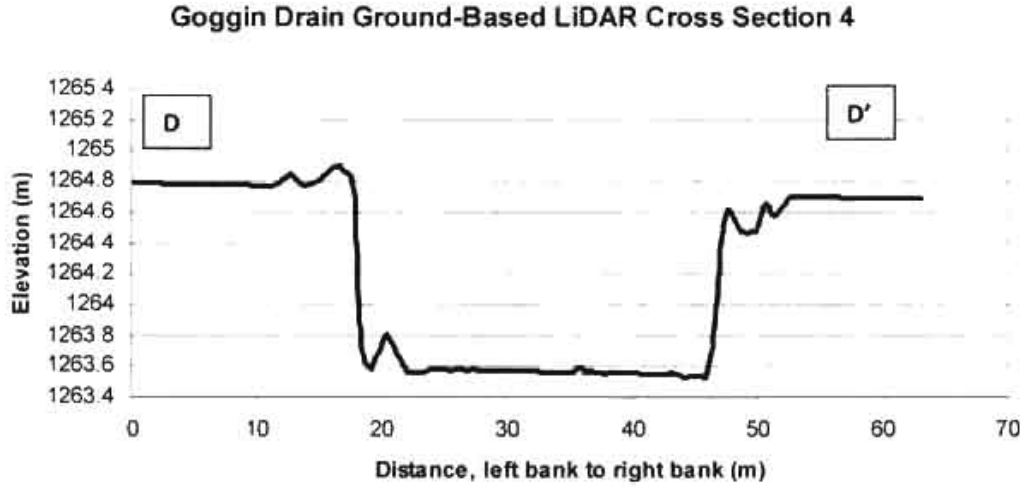

Figure 3.30 continued.

Velocity calculations are displayed in Tables 3.3 and 3.4, and Figure 3.31 shows these calculated velocities plotted against discharge.

For the first geomorphic reach of the Goggin Drain, average cross-sectional velocity was calculated. For the initial calculations, velocities are representative of the discharge in which water depth measurements were made, which was 4.35m^3/s.Velocities were then calculated over the range of discharges measured by the USGS hydrograph.

Velocity of the Goggin Canal was calculated using the method described in Chapter 2. USGS stream gauge data was used to plot gauge height vs. discharge, which was then used to find the gauge height at the time of measurement. The gauge height was assumed to be the water depth, and from this the hydraulic radius and Mannings coefficient of 0.024 were calculated. A velocity of 0.56 m/s was calculated for a discharge of 4.35 m^3/s.

Velocities for the full range of discharges were then calculated. Velocity vs. discharge for both the canal and geomorphic reach 1 of the natural channel are plotted in Figure 3.31. Tables displaying complete data for velocity calculations may be found in Appendix D.

Field Measurement of Velocity, Lee Creek

Tables 3.5 and 3.6 show the velocities calculated for reach 1 and reach 3 of the Lee Creek, along with cross-sectional area, discharge, and the velocity calculated with the Manning equation. Discharge at the time of measurement was ~2.2 m^3/s. Complete field measurements are shown in Appendix E. Also shown are the cross-sectional profiles derived from measuring water depth in increments across the channel.

Table 3.3. Average velocities calculated for each geomorphic reach of the Lee Creek. These calculations correspond to measurements taken on 3/17/08, when the discharge was 0.88 m^3/s.

Reach	Average Width (m)	Average Water Depth (m)	Hydraulic Radius (R)	Slope (m/m)	Mannings Coefficient	Velocity (m/s)	Discharge (m^3/s)
1	14.11	0.45	0.22	1.42E-03	0.099	0.14	0.88
2	5.10	0.75	0.33	1.36E-03	0.076	0.23	0.88
3	12.27	0.48	0.23	4.50E-04	0.053	0.15	0.88

Table 3.4. Average velocities calculated for geomorphic reaches of the Goggin Drain. These calculations correspond to measurements taken on 4/19/09,when the discharge was 4.35 m^3/s.

Reach	Average Width (m)	Average Water Depth (m)	Hydraulic Radius (R)	Slope (m/m)	Mannings Coefficient	Velocity (m/s)	Discharge (m^3/s)
1	30.9	0.42	0.21	4.83E-04	0.020	0.35	4.35
Canal	15.24	0.52	0.25	1.13E-03	0.024	0.56	4.35

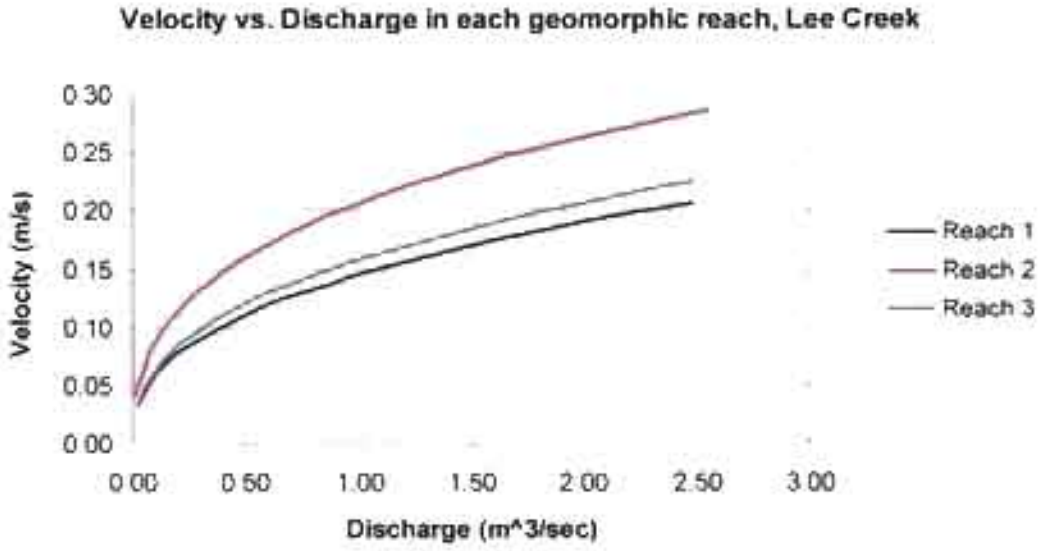

(A)

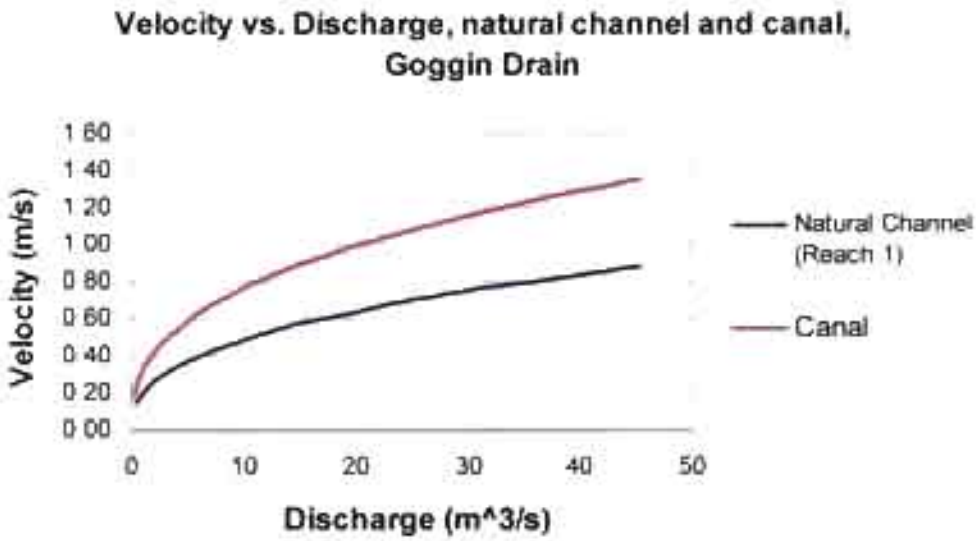

(B)

Figure 3.31. Calculated velocity plotted against the natural range of discharges for both creeks.

Table 3.5. Observed and calculated discharge and velocity for Reach 1, Lee Creek.

Field Velocity Measurement, Lee Creek Reach 1	
Area of cross section	4.91 m^2
Total discharge measured in field	2.20 m^3/s
Average cross-sectional velocity	0.45 m/s
Velocity calculated with Manning Equation	0.20 m/s

Table 3.6. Observed and calculated discharge and velocity for Reach 3, Lee Creek.

Field Velocity Measurement, Lee Creek Reach 3	
Area of cross section	4.68 m^2
Total calculated discharge	2.17 m^3/s
Average cross-sectional velocity	0.46 m/s
Velocity calculated with Manning Equation	0.22 m/s

Empirical Relationships

For the Lee Creek, a meandering stream, empirical relationships compiled by Bridge (2003) were investigated:

1) The relationship between meander length and discharge,

Meander Length (L) = Constant (c) * Discharge (Q) ^ Exponent (x) (Equation 3.1)

where c and x are given and Q is the average discharge of $1.5m^3/s$, according to the Lee Creek gauging station. Table 3.7 shows the results.

2) Relationship between width and discharge,

Width (W) = Constant (c) * Discharge (Q) ^ Exponent (x) (Equation 3.2)

where c and x are given and Q is the average discharge of $1.5m^3/s$, according to the Lee Creek gauging station. Table 3.8 shows the results.

Table 3.7. Relationship between meander length and discharge.

C	Q (m3/s)	x	Theoretical Meander Length (m)	Average Observed Meander Length (m)	Author
49.6	1.5	0.5	60.75	325	Various data sets
65.9	1.5	0.5	80.71	325	Various data sets
65.2	1.5	0.5	79.85	325	Leopold & Wolfman (1957)
166.6	1.5	0.46	200.76	325	Carlston (1965)
61.2	1.5	0.47	74.05	325	Ackers & Charlton (1970)
35.6	1.5	0.63	45.96	325	Ferguson (1975)
35.7	1.5	0.55	44.62	325	Dury (1976)
72.16	1.5	0.49	88.02	325	Mackey (1993)

(Bridge 2003)

Table 3.8. Relationship between width and discharge.

C	Q (m3/s)	x	Theoretical Width (m)	Average Observed Width (m)	Author
8.8	1.5	0.5	10.78	10.74	Inglis (1948)
10.99	1.5	0.46	13.24	10.74	Carlston (1965)
9.81	1.5	0.42	11.63	10.74	Ackers & Charlton (1970)
3.08	1.5	0.54	3.83	10.74	Dury (1976)
4.33	1.5	0.49	5.28	10.74	Mackey (1993)

(Bridge 2003)

3) The relationship between meander length and width,

Meander Length (L) = Constant (c) * Width (W) ^ Exponent (x) (Equation 3.3)

where c and x are given and W is the average measured channel width of 10.74m. Table 3.9 shows the results.

Table 3.9. Relationship between meander length and width.

C	x	Width (m)	Theoretical Meander Length (m)	Average Observed Meander Length (m)	Author
3.03	1	10.74	32.54	325	Inglis (1948)
6.46	1	10.74	69.38	325	Various
7.32	1.1	10.74	99.68	325	Leopold & Wolfman (1957)
11.03	1.01	10.74	121.31	325	Leopold & Wolfman (1960)
10	1.03	10.74	115.33	325	Zeller (1967)
11	1.14	10.74	164.72	325	Ferguson (1975)
10.71	1	10.74	115.03	325	Dury (1976)
7.5	1.12	10.74	107.10	325	Williams (1986)
14.14	0.99	10.74	148.30	325	Mackey (1993)

(Bridge 2003)

CHAPTER 4

DISCUSSION

The Lee Creek and Goggin Drain provide a unique perspective on the complexity and sensitivity of the fluvial system. Although these streams are situated in similar environments and are only a few kilometers apart, their morphologies have evolved very differently and their avulsive behavior is in stark contrast. From analysis of the geomorphology and channel hydraulics of these streams, details that explain these differences emerge.

The Goggin Drain channel form is that of a braided stream with multiple active channels; all portions of the channel are nearly straight and lack well developed meanders. According to Ritter (1986), three factors have the greatest influence on the evolution of a braided pattern: 1) erodible banks, 2) high sediment supply, and 3) variable discharge. The Goggin Drain shows all of these characteristics. The erodibility of the substrate and the high sediment supply is evident in that at least some incision has taken place throughout the study area, with the greatest incision depth (about 1.15 m) occurring in the furthest upstream reach. The total volume of sediment removed due this incision is 5.55×10^5 m^3. The presence of a remnant delta and levees suggest this sediment is stored in the beach zone rather than offshore. This inference, along with the observed variability in discharge documented by the stream hydrograph, suggest that the Goggin Drain is often underfit, meaning that it often fills only a portion of the channel it has carved. The

hydrographs indicate that average discharge may range from nearly no flow in the dry seasons, to high flow with discharges of 40 m^3/s during spring runoff. Normalizing these data to multiples of base flow show that spring runoff regularly reaches ten times the discharge of its base flow, and at maximum may exceed thirty times the volume of base flow. The large volume of sediment removed by incision, along with any sediment transported from upstream, is likely deposited in the channel during times of low discharge, leading to a reduction in channel capacity and braiding.

The Lee Creek has evolved into a more meandering system. From 2001, when the first incised channel form was observed for the Lee Creek, it has taken the form of a single threaded channel that is moderately sinuous (sinuosity $\approx$ 1.2), with meanders forming mostly in the middle and lower reaches of the stream Incision has taken place in these reaches, and a natural nickpoint formed during the lake's regression from its highstand continues to migrate upstream. Incision in this channel is deeper than in the Goggin Drain, over two m in the middle reach, but overall less sediment has been removed ($\sim 3.46 \times 10^5$ m^3). The lack of remnant deltas observed in this system suggests that the majority of this sediment has been flushed offshore. Although the Lee Creek generally has a much smaller discharge volume than the Goggin Drain, reaching a maximum of about 2.5m^3/s , it also has a steadier flow pattern, with a ratio of spring runoff to base flow at about 1.6. In the modern evolution of the channel (2001 to present), available data suggest that this stream does not reach flows as low as those observed in the Goggin Drain. Therefore sediment is not as likely to be deposited within the channel.

Along with volume of discharge, these two systems also differ in the magnitude of the calculated cross-sectional velocities, considering the results of the Manning

equation calculations. The highest calculated velocity for the Lee Creek is ~ 0.29 m/s. This creek shares similar velocities in its first and third reaches, which are the unincised upper region and the delta, respectively. Both of these reaches are wide and shallow and have small incision depths (~0.8 m) in comparison with the middle reach (~2.0 m). This narrow, deeply incised middle reach has faster cross sectional velocities at all discharges. Because the natural range of discharges for the Goggin Drain is an order of magnitude higher than the Lee Creek, it can accommodate higher flow velocities of up to 1.40 m/s in the channelized canal and up to 0.85 m/s in the natural reaches downstream.

This disparity in velocity implies a difference in erosional power of the two streams, which is potentially manifested in the contrasting styles in which incision observed. Nickpoints continue to migrate headward in the Lee Creek, while the Goggin Drain has a flatter longitudinal profile with no observed nickpoints. A more detailed study of how velocity affects shear stress along the channel bed is needed to relate streamflow, channel erosion and channel form.

In addition to geomorphic differences, the avulsive behavior of the two systems varies historically. From 1965 to 2006, three full avulsions of large reaches of the Goggin Drain are observed, while Lee Creek has remained more stable with no major avulsions observed. In the case of Lee Creek, the fluvial architecture is mainly affected by lake transgressions and regressions, as this channel has not recently avulsed. In contrast, because the Goggin drain has been much more actively adjusting, its channel has moved across the lake bed with each avulsion in addition to the movements associated with lake level changes.

Findings thus far suggest two styles of avulsion in the Goggin Drain: 1) an allogenic response forced by changes in lake level, and 2) an autogenic response resulting from channel hydraulics of the system. In both cases, aggradation pushes the system toward its avulsion threshold, and flooding is the likely trigger.

In the case of an allogenic response, the system is pushed toward its avulsion threshold by either a rise or fall in base level - both scenarios may result in aggradation. In the case of a transgression, the result will be a decrease in stream gradient accompanied by aggradation (Miall 1996). The active channels may become choked with sediment, which reduces their carrying capacity and increases the likelihood of an avulsion. A regression of the system may have a similar effect. As discussed above, laboratory experiments (Jones and Schumm 1999) and field data (Morovosa and Smith 1999) have shown that when a regression occurs and the newly exposed land area is a flat lake bed, the overall gradient of the channel is reduced, again resulting in aggradation and a shift toward the avulsion threshold. In both cases, the frequency of flooding of the Goggin Drain is interpreted as the most likely trigger for the avulsion.

Evidence for this style of avulsion is derived from geomorphic analysis of the region, longitudinal profiles, and hydrographs of both the stream and the lake. Airborne LiDAR images of the field site show the presence of a remnant delta, evidence that aggradation and sediment deposition has taken place. The longitudinal profile of the stream channel and its bank shows that gradient decreases in the basinward direction, indicating that aggradation due to regression may be possible. Additionally, the lake hydrograph shows that avulsion periods have been characterized by either rises or falls in lake level. The 1971-1977 avulsion took place during a steady rise in lake levels, while

both the 1989-1997 avulsion and the 2001-2005 avulsion took place during periods characterized by an initial regression followed by steadying (Figure 3.5). An examination of the Goggin Drain/Surplus Canal hydrograph during these same time periods shows variation in the magnitude of flooding that took place during these periods. While only the 1989-1997 avulsion was accompanied by notably high discharges, hydrograph analyses of other documented modern avulsions show that such an event does not necessarily occur at the highest point of discharge (Ethridge et al. 1999).

The second potential style of avulsion that can be interpreted is a purely autogenic response dictated by the geomorphology and channel hydraulics of the system. Avulsion is an integral part of the braiding process (Miall 1996), so all the geomorphic factors that have affected the evolution of the Goggin Drain channel form (sediment supply, frequency of flooding, etc.) may adequately explain its avulsive behavior. The channel hydraulics of the system may also play a role. When considering this possibility, it is important to note that the avulsion of the Goggin Drain takes place from the point at which the channel is released from confinement, at the transition from an engineered canal to a natural channel. This is also the point from which the remnant delta appears to originate. As displayed in Figure 3.30, a comparison of the calculated velocities between these two reaches indicates that for the full range of stream discharges, flow within the canal is always faster than flows than within the natural portion of the channel. These observations suggest that throughout the range of discharges of the Goggin Drain, deposition may always take place near this point. It follows that avulsions at or near this point are autogenic responses associated with channel blockage due to aggradation. In this case, however, there is no downstream external forcing to the system which would

push the stream to an avulsion threshold. In this scenario, the downstream decrease in velocity would exist during times of regression, transgression and stability; base level changes do not affect this relationship, therefore channel hydraulics are the more important factor controlling avulsion in these streams. Further evidence supporting an autogenic response to avulsion may be drawn from the fact that while the Lee Creek has been subjected to the same downstream forcing, its channel has remained stable. The intrinsic properties which may promote avulsions in the Goggin Drain are not present in the Lee Creek: it is not released from confinement, and it does not have a variable discharge. However, the main limitation in comparing these two systems is the Lee Creek's low discharge early in the study period. Between 1965 and 1982, average discharge was only about 0.1 m^3/s, Evidently this was not enough erosional power to form an incised channel, as a single channel form was not observed until 2001. Because true channel avulsions could not occur until after this time, the observation period for avulsions of the Lee Creek has effectively been much shorter.

The recent incision of the Lee Creek may also explain why observed meander lengths are considerably longer than those predicted by empirical relationships. While theoretical meander lengths are predicted to be about 100 m, the average observed meander length is about 325 m. The low sinuosity observed may be a sign that the channel form is still reaching equilibrium, and over time erosion will produce tighter meanders.

Another limitation of this study should be noted: the channels within the study site are not entirely natural, and anthropogenic factors control much of the system, especially in the areas upstream of the study sites that are urban or industrial. The Goggin

Drain has been unnaturally channelized for most of its course, and its volume of discharge is controlled. The source of the Lee Creek is an engineered wetland. However, there is inherent value in studying these systems, as many natural analogies can be made to the unnatural elements of the systems, such as structural controls, and discharge patterns are similar to those of braided systems, etc.

Airborne and terrestrial LiDAR has been an excellent tool for the qualitative geomorphic assessment of the area of interest, due to the detail of the DEMs produced. Modern geomorphic and sedimentary features not always visible to the naked eye were more easily identified on the high resolution DEMS, particularly remnant channels, deltas and levees. Because these features can be linked to historical aerial images, the end result is a better understanding of form and process in the fluvio-lacustrine system. LiDAR was especially useful tool in this study due to the low relief of the topography of the study area.

The LiDAR-derived DEMs are useful in the study of modern channel hydraulics. As discussed in Chapter 2, the data were used to calculate average cross-sectional velocity at several points along the stream. Velocities measured in the field were about twice as fast as the calculated velocities. A possible explanation may be that the square channel assumption in the Manning calculations is not accurate, especially in the reach that was not incised, as the channel beds here tend to be more rounded. Because the velocity was only measured at one point for each reach, and because of the natural range of velocities observed within stream channels, the calculated velocity is believed to be reasonable when compared to the measured velocity.

For most portions of the channels, field work was required to measure the incision depth of the channels, due to the fact that the laser pulses cannot penetrate water in the channels. However, this need was eliminated for the portion of the Goggin Drain which also was surveyed with ground-based equipment. Knowing the gradient of both the channel bed and the water surface allowed for velocity to be calculated based on the LiDAR images alone. Having surveys of both the water-filled and empty channel also has the potential for use in more detailed modeling studies, such as 2D and 3D flow calculations and sediment transport models. However, the availability of this type of data would be mostly limited to semiarid climates, where ephemeral stream systems are most common.

Some additional challenges associated with using LiDAR images affected this research. The sparse data returns over water can be problematic when working with streams, and creating cross-sectional and longitudinal profiles may require additional processing as a result, as was required with the data used in this study. Also, assessing the morphology of the stream banks was locally hampered where dense riparian vegetation blocked the return signal of the laser pulses; even with a "bare earth" model, thick vegetation cannot be erased in the DEMs.

CHAPTER 5

CONCLUSIONS

Two possible styles of avulsion are interpreted: an allogenic response to changing base level and an autogenic response related to channel hydraulics. These avulsions and potential causal mechanisms such as base level changes and flooding events have been well documented through aerial imagery, LiDAR data and hydrographs. However, despite the availability of detailed information, it is not possible to definitively attribute channel avulsions to allogenic forcing factors rather than to autogenic responses intrinsic to the stream system.

Similarly, hydraulic properties of the streams appear to play a stronger role in channel evolution than other environmental factors. Although the Lee Creek and the Goggin Drain are situated only a few kilometers apart and share similar gradients, substrates, vegetation patterns etc, and are subjected to the same changes in lake level, their forms have evolved very differently. Differences in discharge patterns are likely the most influential factor in the meandering form of the Lee Creek and the braiding of the Goggin Drain.

Airborne and terrestrial LiDAR data have proven to be excellent tools for geomorphic analysis of sedimentary structures in study area. In a low gradient environment such as the beaches of the Great Salt Lake, many features would likely go

unnoticed without accurate DEMs. However, due to the gaps in data and errors produced over water, LiDAR is not an ideal tool for studying active streams channels or shorelines.

Fluvial systems are clearly sensitive to both internal and external changes. However, more research is needed in order to isolate each forcing in order to determine its affects on geomorphology and stratigraphy. This study emphasizes the need for caution when attempting to attribute channel avulsions to allogenic factors, especially base level changes. This is especially important when assessing ancient systems, when details are inferred from the rock record or boreholes, and no direct information on channel hydraulics is available. Analysis of the Lee Creek and Goggin Drain serves as further evidence of the complexity of fluvial processes.

APPENDIX A

GOGGIN DRAIN-SURPLUS CANAL CORRELATION

Figures A.1 and A.2 display average monthly discharges during spring runoff, as recorded by USGS gauging stations on the Goggin Drain and Surplus Canal. Plotting peak discharges for each stream against each other yields nearly a one-to-one relationship.

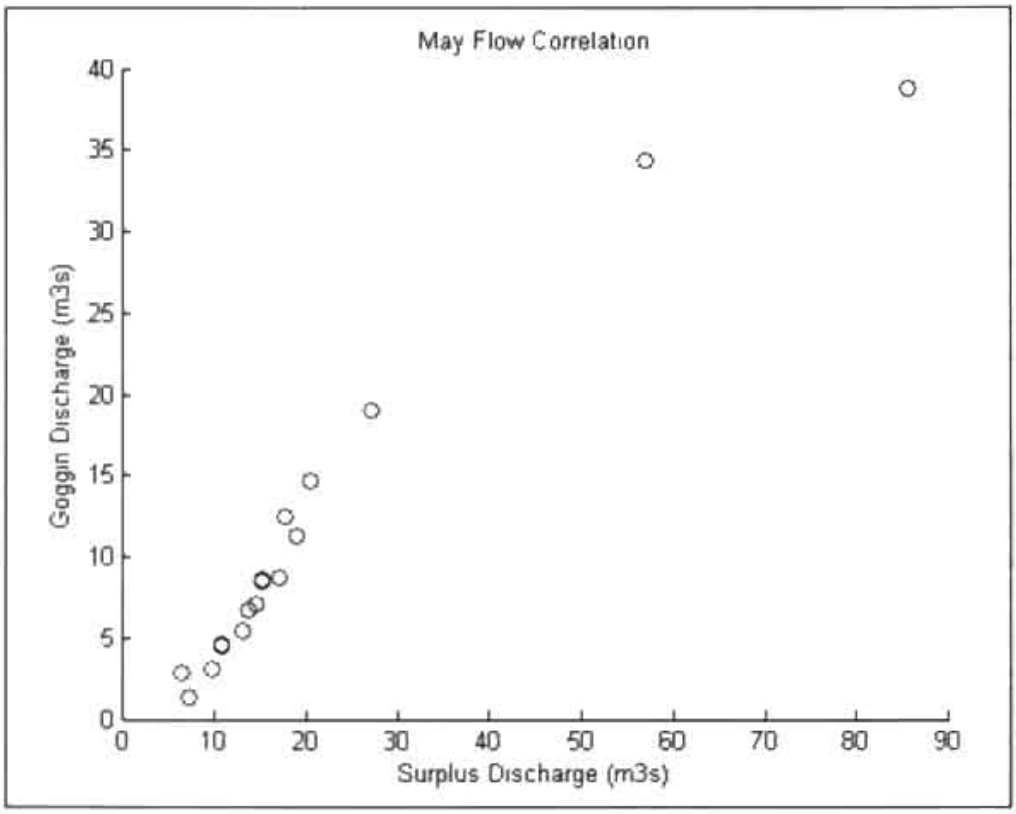

Figure A.1. May flow correlation between the Goggin Drain and Surplus Can.

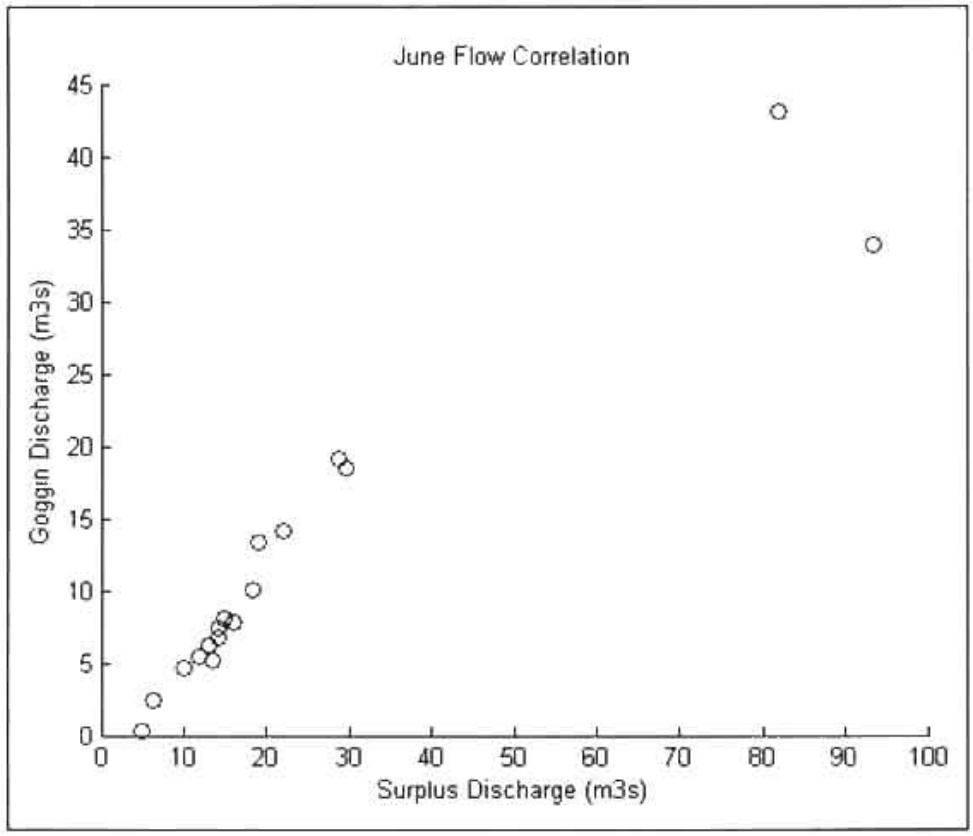

Figure E.2. June flow correlation between the Goggin Drain and Surplus Canal.

APPENDIX B

CHANNEL MORPHOLOGY DATA

Table B.1. Lee Creek channel measurements. Distance from shoreline, incision measurements, channel width, and depth.

Waypoint	Distance from shore (m)	Distance to next waypoint downstream (m)	Channel width (m)	Total incision (m)	Incision from bank to water surface (m)	Water Depth (m)
1	2854.80	122.40	26.20	0.35	0.11	0.24
2	2732.40	141.50	21.10	0.96	0.43	0.53
3	2590.90	201.80	15.10	0.73	0.34	0.40
4	2389.10	56.90	9.90	0.78	0.37	0.41
5	2332.20	56.60	4.60	1.45	0.49	0.96
6	2275.60	138.10	10.60	0.58	0.27	0.30
7	2137.50	217.30	11.30	0.98	0.67	0.30
8	1920.20	118.00	4.90	1.49	1.04	0.46
9	1802.20	173.60	4.50	2.13	1.34	0.79
10	1628.60	121.30	5.60	1.83	1.34	0.49
11	1507.30	424.70	5.50	2.65	1.71	0.94
12	1082.60	238.60	5.00	2.04	0.98	1.07
13	844.00	413.00	9.30	0.79	0.40	0.40
14	431.00	326.70	9.50	1.13	0.40	0.73
15	104.30	104.30	18.00	0.46	0.15	0.30

Table B.2. Goggin Drain channel measurements. Distance from shoreline, incision measurements, channel width and depth. Values followed by an asterix were unattainable due to field conditions, and were therefore estimated based on field observations and average values of measurements from nearby locations.

Waypoint	Distance from shore (m)	Distance to next waypoint downstream (m)	Channel width (m)	Total incision (m)	Incision from bank to water surface (m)	Water Depth (m)
1	1952.6	247.3	32.8	1.34*	0.94	0.40*
2	1705.3	140.9	18.0	1.19*	0.79	0.40*
3	1564.4	133.5	27.7	1.1	0.70	0.40
4	1430.9	143.0	30.7	1.15	0.88	0.27
5	1287.9	175.0	36.5	1.2	0.61	0.59
6	1112.9	163.4	30.0	0.8	0.61	0.19
7	949.5	322.4	43.6	0.92*	0.52	0.40*
8	627.1	176.1	34.4	0.72*	0.32	0.40*
9	451.0	107.5	24.9	0.86*	0.46	0.40*
10	343.5	216.4	30.5	0.74*	0.34	0.40*
11	127.1	127.1	35.4	0.46*	0.26	0.20*

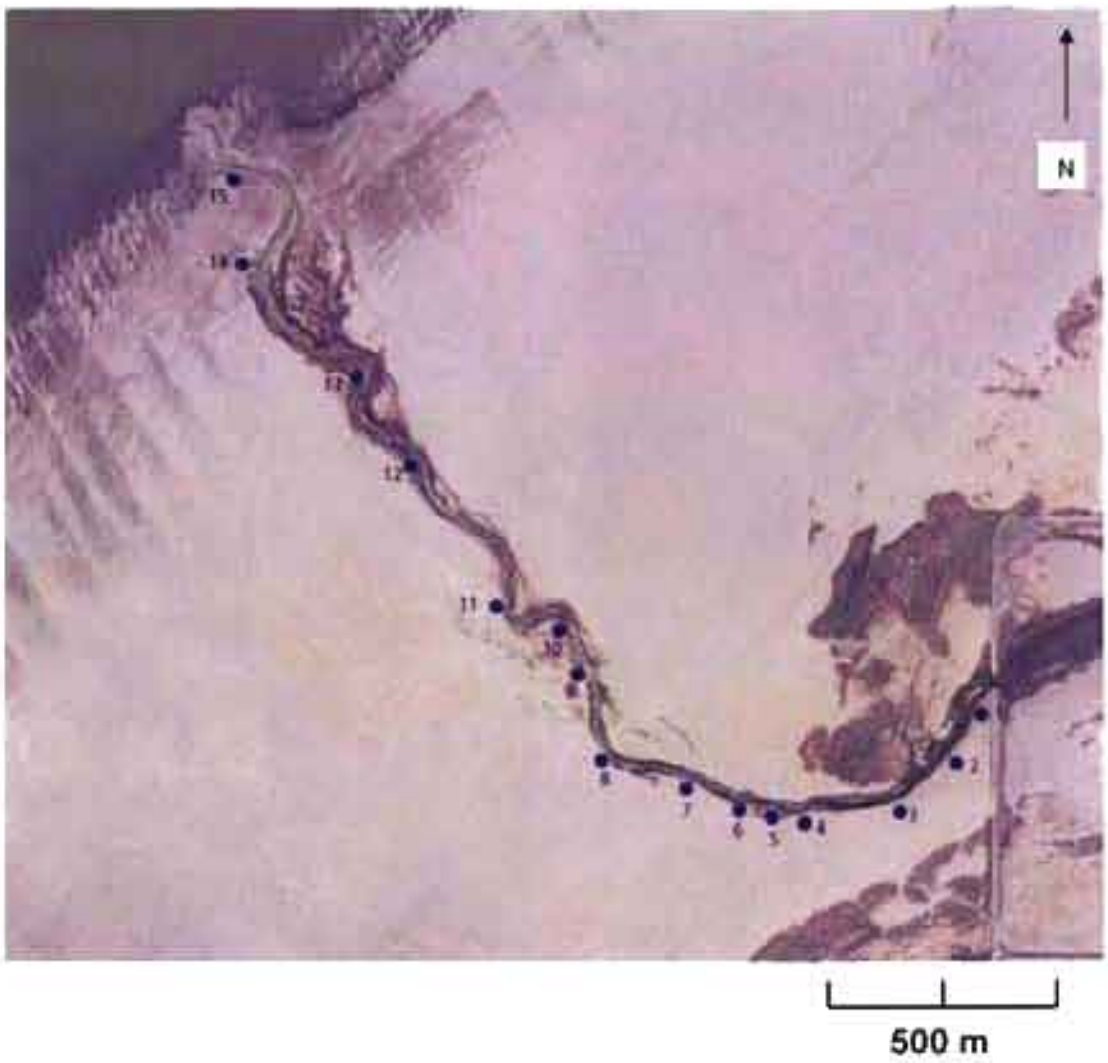

Figure B.1. Map displaying measurement waypoint locations, Lee Creek.

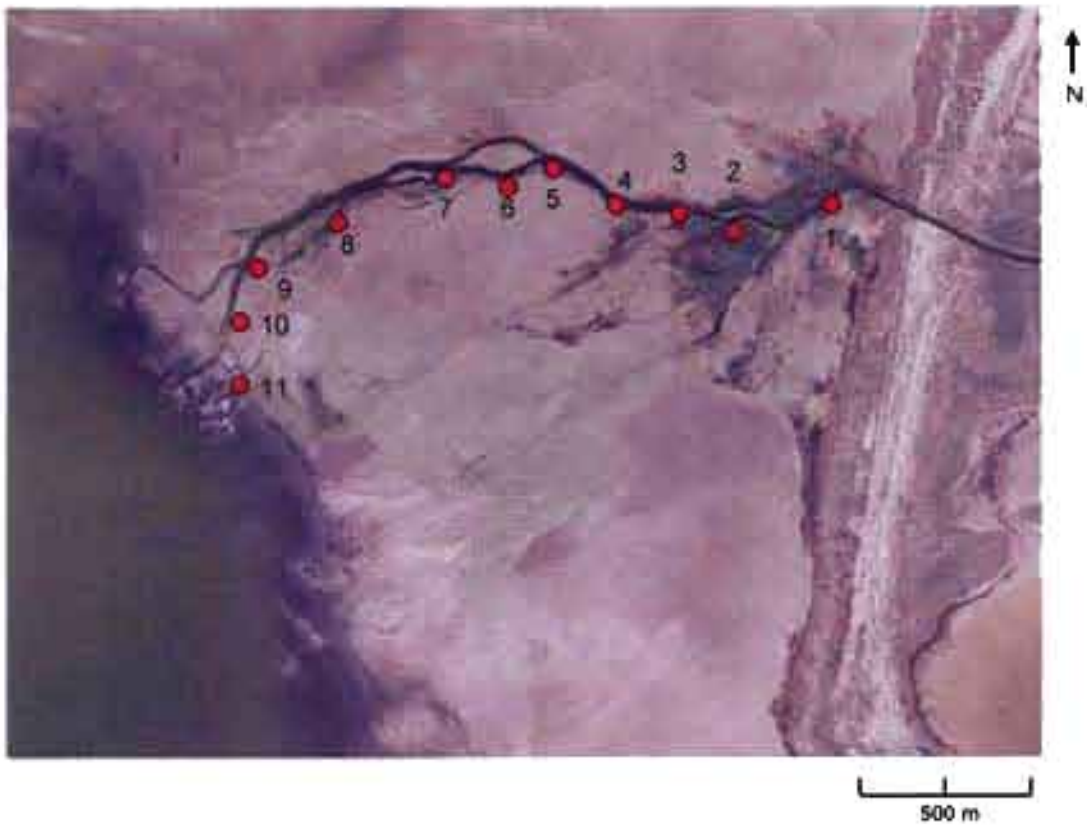

Figure B.2. Map displaying measurement waypoint locations, Goggin Drain

APPENDIX C

SEDIMENT VOLUME CALCULATIONS

Table C.1. Calculation of total sediment volume removed by incision, Lee Creek.

Waypoint	Surface area of downstream reach (m^2)	Total incision (m)	Volume of downstream reach (area*incision) (m^3)	Total volume of sediment removed by incision (m^3)
1	2784.6	0.35	976.0	34593.7
2	2174.9	0.96	2088.1	
3	2465.0	0.73	1803.2	
4	479.0	0.78	372.3	
5	500.7	1.45	725.0	
6	1169.0	0.58	677.0	
7	2049.7	0.98	1999.2	
8	808.7	1.49	1207.8	
9	540.9	2.13	1154.1	
10	1198.5	1.83	2191.9	
11	3138.0	2.65	8321.1	
12	2116.3	2.04	4321.8	
13	4320.1	0.79	3423.6	
14	3892.6	1.13	4389.9	
15	2062.0	0.46	942.7	

Table C.2. Calculation of total sediment volume removed by incision, Goggin Drain.

Waypoint	Area of downstream reach (m^2)	Total incision (m)	Volume of downstream reach (area*incision) (m^3)	Total volume of sediment removed by incision (m^3)
1	4858.1	1.34	6533.6	55524.3
2	2517.6	1.19	3002.1	
3	3864.3	1.10	4250.8	
4	3901.5	1.15	4486.7	
5	6337.2	1.20	7604.6	
6	5949.8	0.80	4759.9	
7	11334.4	0.92	10406.8	
8	6073.0	0.72	4372.8	
9	3835.1	0.86	3287.4	
10	6054.5	0.74	4451.8	
11	5157.7	0.46	2367.8	

APPENDIX D

MANNING EQUATION DATA

Table D.1. Velocity calculated along each reach of the Lee Creek on 3/17/08. According to the USGS gauging station, the discharge was 0.88 m^3/s.

Waypoint	Channel width (m)	Water depth (m)	Hydraulic Radius R	Slope (m/m)	Roughness coefficient	Velocity (m/s)	Discharge (m^3/s)
1	26.2	0.24	0.12	9.32E-04	0.05	0.14	0.88
2	21.1	0.53	0.26	9.32E-04	0.16	0.08	0.88
3	15.1	0.40	0.19	9.32E-04	0.07	0.15	0.87
4	9.9	0.41	0.20	2.53E-03	0.08	0.21	0.87
5	4.6	0.96	0.40	1.53E-03	0.11	0.20	0.85
6	10.6	0.30	0.15	1.53E-03	0.04	0.27	0.88
7	11.3	0.30	0.15	1.53E-03	0.04	0.26	0.88
8	4.9	0.46	0.21	1.53E-03	0.04	0.39	0.86
9	4.5	0.79	0.34	1.53E-03	0.08	0.25	0.88
10	5.6	0.49	0.22	2.21E-03	0.05	0.32	0.88
11	5.5	0.94	0.40	1.06E-03	0.11	0.17	0.88
12	5.0	1.07	0.44	2.72E-04	0.06	0.16	0.86
13	9.3	0.40	0.19	2.72E-04	0.02	0.24	0.87
14	9.5	0.73	0.34	5.38E-04	0.09	0.13	0.89
15	18.0	0.30	0.15	5.38E-04	0.04	0.16	0.88

Table D.2. Velocity calculated along each reach of the Goggin Drain on 4/18/08. According to the USGS gauging station, the discharge was 4.35 m^3/s.

Waypoint	Channel width (m)	water depth (m)	Hydraulic Radius R	Slope (m/m)	Roughness coefficient	Velocity (m/s)	Discharge (m^3/s)
3	29.3	0.40	0.20	3.07E-04	0.016	0.37	4.33
4	29.6	0.27	0.13	3.07E-04	0.0084	0.55	4.35
5	34.0	0.59	0.29	9.42E-04	0.062	0.22	4.35
6	44.2	0.19	0.09	3.77E-04	0.01	0.52	4.34
Average	30.9	0.42	0.21	4.83E-04	0.020	0.35	4.34

In order to calculate velocity within the Goggin Drain canal, USGS field measurement of gauge heights at given discharges were first plotted. Gauge height is assumed to be equivalent to water depth. This plot was then overlain with the curve representing calculated Manning velocity vs. discharge (Figure D.1). Inputs were derived from LiDAR data. The one unknown variable, channel roughness (n), was adjusted until the curve matched the plotted points. Then, because all variables for the Manning equation are known, velocity can be calculated for the full range of discharge in the Goggin canal.

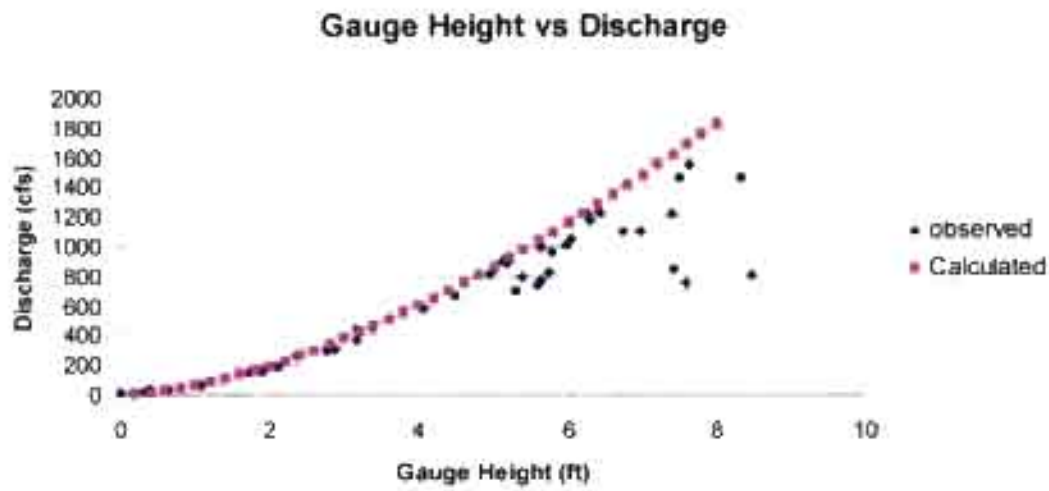

Figure D.1 Observed and calculated gauge height vs. discharge, Goggin Drain Canal.

APPENDIX E

FIELD VELOCITY MEASUREMENTS

Table E.1. Data used to calculate average cross-sectional velocity in Lee Creek geomorphic reach 1.

Distance (m)	Depth(m)	Revolutions	Time (s)	V at point (m/s)	Area (m^2)	Q (m^3/s)
0.0	0.00				0.04	0.01
0.6	0.12	23	45	0.16	0.07	0.01
1.2	0.17	42	45	0.28	0.10	0.03
1.8	0.24	50	45	0.33	0.15	0.05
2.4	0.30	58	45	0.39	0.19	0.07
3.0	0.34	64	45	0.43	0.20	0.09
3.7	0.37	65	45	0.43	0.22	0.10
4.3	0.40	70	45	0.46	0.24	0.11
4.9	0.43	79	45	0.52	0.26	0.14
5.5	0.46	77	45	0.51	0.28	0.14
6.1	0.49	83	45	0.55	0.30	0.16
6.7	0.49	82	45	0.54	0.30	0.16
7.3	0.49	83	45	0.55	0.30	0.16
7.9	0.49	75	45	0.50	0.30	0.15
8.5	0.46	81	45	0.54	0.28	0.15
9.1	0.46	80	45	0.53	0.28	0.15
9.8	0.43	72	45	0.48	0.26	0.12
10.4	0.40	69	45	0.46	0.24	0.11
11.0	0.34	55	45	0.37	0.20	0.08
11.6	0.24	51	45	0.34	0.15	0.05
12.2	0.21	50	45	0.33	0.13	0.04
12.8	0.18	48	45	0.32	0.11	0.04
13.4	0.18	49	45	0.33	0.11	0.04
14.0	0.15	51	45	0.34	0.09	0.03
14.6	0.12	20	45	0.14	0.07	0.01
15.2	0.00				0.04	0.01
				Sum	4.91 m^2	2.20 m^3/s

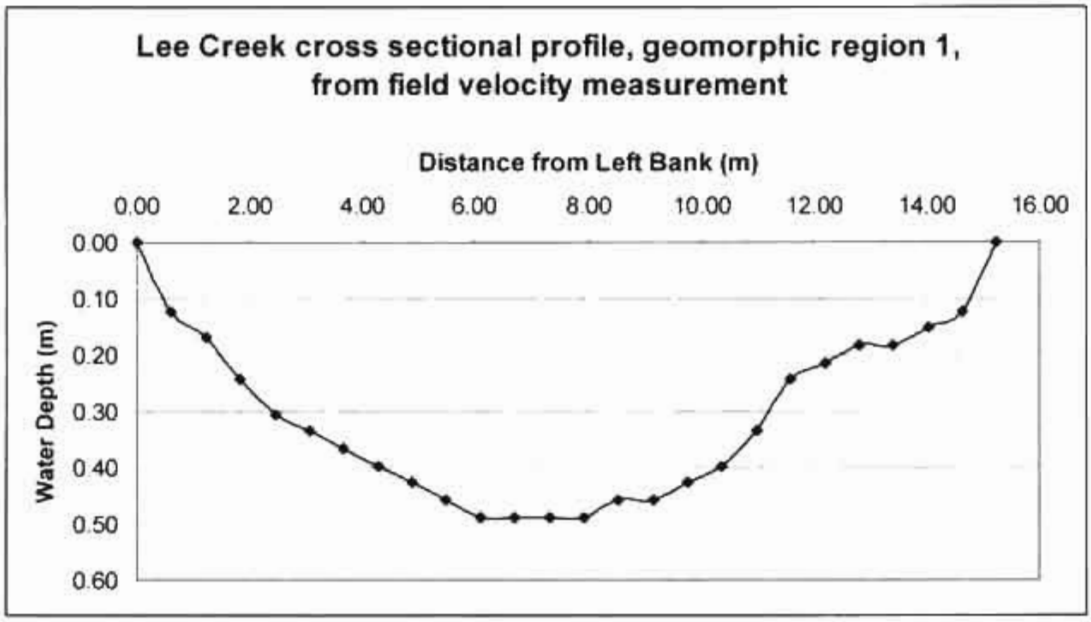

Figure E.1. Cross sectional profile created from field velocity measurements, Lee Creek geomorphic reach 1.

Table E.2. Data used to calculate average cross-sectional velocity in Lee Creek geomorphic reach 3.

Distance (m)	Depth (m)	Revolutions	Time (s)	V at point (m/s)	Area (m^2)	Q (m3/s)
0.00	0.00				0.05	0.02
0.61	0.15	45	45	0.30	0.09	0.03
1.22	0.21	48	45	0.32	0.13	0.04
1.83	0.27	59	45	0.39	0.17	0.07
2.44	0.30	62	45	0.41	0.19	0.08
3.05	0.34	58	45	0.39	0.20	0.08
3.66	0.34	64	45	0.43	0.20	0.09
4.27	0.34	64	45	0.43	0.20	0.09
4.88	0.34	59	45	0.39	0.20	0.08
5.49	0.30	68	45	0.45	0.19	0.08
6.10	0.34	73	45	0.48	0.20	0.10
6.71	0.34	70	45	0.46	0.20	0.10
7.32	0.34	75	45	0.50	0.20	0.10
7.93	0.34	70	45	0.46	0.20	0.10
8.54	0.37	80	45	0.53	0.22	0.12
9.15	0.37	77	45	0.51	0.22	0.11
9.76	0.40	79	45	0.52	0.24	0.13
10.37	0.37	81	45	0.54	0.22	0.12
10.98	0.40	84	45	0.56	0.24	0.13
11.59	0.40	82	45	0.54	0.24	0.13
12.20	0.49	84	45	0.56	0.30	0.17
12.80	0.49	82	45	0.54	0.30	0.16
13.41	0.27	37	45	0.25	0.11	0.03
13.81	0.00				0.05	0.02
				Sum	4.68	2.17

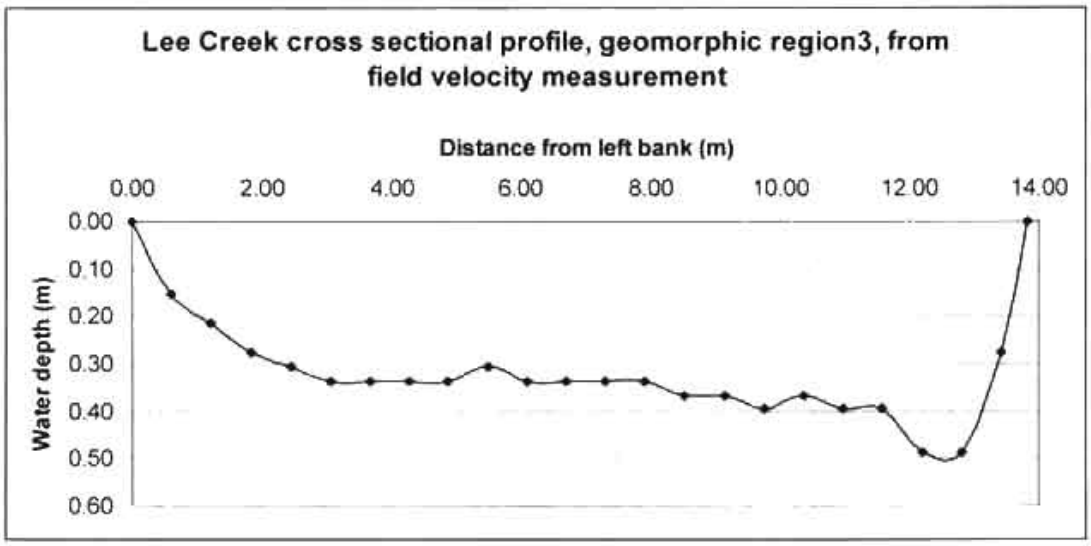

Figure E.2. Cross sectional profile created from field velocity measurements, Lee Creek geomorphic reach 1.

REFERENCES

Aslan, A. and M.D. Blum, 1999, Contrasting styles of Holocene avulsion, Texas Gulf Coastal Plain, U.S.A.: Fluvial Sedimentology VI, Special Publications of the International Association of Sedimentologists, v. 28, p. 193-210.

Blair, T.C. and J.G. McPherson, 1994, Historical adjustments by Walker River to lake-level fall over a tectonically tilted half-graben floor, Walker Lake Basin, Nevada: Sedimentary Geology, v. 92, no. 1-2, p. 7-16.

Bloom, A. L., 1998, Geomorphology: A Systematic Analysis of Late Cenozoic Landforms: Prentice-Hall, Upper Saddle River, NJ, 482 p.

Bridge, J.S, 2003, Rivers and Floodplains: Forms, Processes and Sedimentary Record: Blackwell Publishing, Malden, Mass, 514 p.

Bristow, C.S., 1999, Gradual avulsion, river metamorphasis and reworking by underfit streams: a modern example from the Brahmaputra River in Bangladesh and a possible ancient example from the Spanish Pyrenees: Fluvial Sedimentology VI, Special Publications of the International Association of Sedimentologists, v. 28, p. 221-231.

Burns, A.B. et al., 1997, Fluvial response in a sequence stratigraphic framework; example from the Montserrat fan delta, Spain: Journal of Sedimetary Research, v. 67, p. 311-321.

Ethridge et al., 1999, Avulsion and crevassing in the sandy, braided Niobara River: complex response to base level rise and aggradation: Fluvial Sedimentology VI, Special Publications of the International Association of Sedimentologists, v. 28, p. 179-191.

Ethridge, F.G. et al., 2005, The morphological and stratigraphical effects of base level change: a review of experimental studies: Fluvial Sedimentology VII, Special Publications of the International Association of Sedimentologists, v. 35, p. 213-241.

Gibling, M. R., 2006, Width and thickness of fluvial channel bodies and valley fills in the geological record: a literature compilation and classification: Journal of Sedimentary Research, v. 76, p. 731-770.

Hart, B.S., and B.F. Long, 1996, Forced regressions and lowstand deltas: Holocene Canadian examples: Journal of Sedimentary Research, v. 66. no. 4, p. 820-829.

Hassan, M. A., and M. Klein, 2002, Fluvial adjustment of the Lower Jordan River to a drop in the Dead Sea level: Geomorphology, v. 45, no. 1, p. 21-33.

Heller, P.L., and C. Paola, 1996, Downstream changes in alluvial architecture: An exploration of controls on channel-stacking patterns: Journal of Sedimentary Research, v. 66, no. 2, p. 297-306.

Heller, P. L. et al., 2001, Geomorphology and sequence stratigraphy due to slow and rapid base-level changes in an experimental subsiding basin (XES 96-1): AAPG Bulletin, v. 85, no. 5, p. 817-838.

Hickson,, T.A. et al., 2005, Experimental test of tectonic controls on three-dimensional alluvial facies architecture: Journal of Sedimentary Research, v. 75, p. 710-722.

Hilldale, R.C., and D. Raff, 2008, Assessing the ability of airborne LiDAR to map river bathymetry: Earth Surface Processes and Landforms, v. 33, p. 773-783.

Intermountain Region Digital Image Archive Center (IRDIAC), earth.gis.usu.edu/

Jones, L.S., and S.A. Schumm, 1999, Causes of avulsion: Fluvial Sedimentology VI, Special Publications of the International Association of Sedimentologists, v. 28, p. 171-178.

Keighley et al., 2003, Sequence stratigraphy in lacustrine basins: A model for part of the Green River Formation (Eocene), southwest Uinta basin, Utah, U.S.A.: Journal of Sedimentary Research, v. 73, no. 6, p. 987-1006.

Kraus, M.J., and T.M. Wells, 1999, Recognizing avulsion deposits in the ancient stratigraphic record: Fluvial Sedimentology VI, Special Publications of the International Association of Sedimentologists, v. 28, p. 251-268.

Kroonenberg, S.B. et al., 1997, The wandering of the Volga delta: a response to rapid Caspian sea-level change: Sedimentary Geology, v. 107, p. 189-209.

Lin, C. et al., 2001, Sequence architecture, depositional systems, and controls on development of lacustrine basin fills in part of the Erlian Basin, northeast China: AAPG Bulletin, v. 85, no. 11, p. 2017-2043.

McCuen, R.C., 1998, Hydrologic Analysis and Design: Prentice Hall, Upper Saddle River, N.J, 814 p.

Miall, A.D., 1996, The Geology of Fluvial Deposits; Sedimentary Facies, Basin Analysis, and Petroleum Geology: Springer –Verlag Berlin Heidelberg New York, 582 p.

Morovoza, G.S., and N.D. Smith, 1999, Holocene avulsion history of the lower Saskatchewan fluvial system, Cumberland Marshes, Saskatchewan-Manitoba: Fluvial Sedimentology VI, Special Publications of the International Association of Sedimentologists, v. 28, p. 231-249.

Moskal, L.M., 2008, LiDAR Fundamentals: Workshop on site-scale applications of LiDAR on forest lands in Washington, Center for Urban Horticulture, University of Washington, Jan. 3.

Ritter, D.F.,1986, Process Geomorphology: Wm. C. Brown Publishers, Dubuque, Iowa, 603 p.

Sanders, L.L., 1998, A Manual of Field Hydrogeology: Prentice Hall, Upper Saddle River, N.J, 381 p.

Schumm, S.A, 1993, River responses to base level change: Implications for sequence stratigraphy: Journal of Geology, v. 101, p. 279-294.

Schumm, S.A., and L.S. Jones, 1999, Causes of Avulsion: an Overview: Fluvial Sedimentology VI, Special Publications of the International Association of Sedimentologists, v. 28, p. 171-178.

Sinha, R. et al., 2005, Sedimentology and avulsion patterns of the anabranching Baghmati River in the Himalayan foreland basin, India: Fluvial Sedimentology VII, Special Publications of the International Association of Sedimentologists, v. 35, p. 181-196.

Snyder, N.P., 2009, Studying stream morphology with airborne laser elevation data: Eos, Transactions, American Geophysical Union, v. 90, no. 6, p. 45-46.

Stouthamer, E., and H. J. A. Berendsen, 2000, Factors controlling the Holocene avulsion history of the Rhine-Meuse delta (The Netherlands): Journal of Sedimentary Research, v. 70, no. 5, p. 1051-1064.

Stouthamer, E., and H. J. A. Berendsen, 2001, Avulsion frequency, avulsion duration and interavulsion period of the Holocene channel belts of the Rhine-Meuse Delta, The Netherlands: Journal of Sedimentary Research, v. 71, p. 589-598.

Stouthamer, E., and H. J. A. Berendsen, 2007, Avulsion: The relative roles of autogenic and allogenic processes: Sedimentary Geology, v. 198, p. 309-325.

Thoma et al., 2005. Airborne laser scanning for riverbank erosion assessment: Remote Sensing of the Environment, v. 95, p. 493-501.

USGS Utah Water Science Center, http://ut.water.usgs.gov/greatsaltlake/.

The Utah Automated Geographic Reference Center (AGRC). http://agrc.its.state.ut.us/